age

1. Report No. FHWA/TX-94+1244-8	2. Government Accession No.	3. R

4. Title and Subtitle EFFECTS OF AGGREGATE BLENDS ON THE PROPERTIES OF PORTLAND CEMENT CONCRETE PAVEMENTS	5. Report Date August 1994
	6. Performing Organization Code
7. Author(s) Terry Dossey, B. F. McCullough, and Abigail Dumas	8. Performing Organization Report No. Research Report 1244-8
9. Performing Organization Name and Address Center for Transportation Research The University of Texas at Austin 3208 Red River, Suite 200 Austin, Texas 78705-2650	10. Work Unit No. (TRAIS)
	11. Contract or Grant No. Research Study 0-1244
12. Sponsoring Agency Name and Address Texas Department of Transportation Research and Technology Transfer Office P. O. Box 5051 Austin, Texas 78763-5051	13. Type of Report and Period Covered Interim
	14. Sponsoring Agency Code

15. Supplementary Notes

Study conducted in cooperation with the U.S. Department of Transportation, Federal Highway Administration.
Research study title: "Evaluation of the Performance of Texas Pavements Made with Different Coarse Aggregates"

16. Abstract

Although recent studies have shown that pavement performance does vary by aggregate type, current portland cement concrete pavement design tools do not fully incorporate aggregate properties into the design process. Aggregate characteristics shown to affect pavement performance include strength, thermal properties, and shrinkage properties. The objective of this study was to investigate the material properties of crushed limestone and siliceous river gravel, two aggregates predominantly used in current pavement construction, and to determine a relationship between the properties of single-aggregate concrete and concrete made with predetermined blends of limestone and gravel. This report continues the work of Project 422/1244, which was limited to single-aggregate concretes. Additional models were developed to predict concrete properties of blended aggregate concrete for use in the design tools, CRCP and JRCP, described in previous 422/1244 reports. A computer program, CHEM2, was developed, which allows the pavement designer to estimate the material properties of concrete from an inexpensive chemical test. CHEM2 also predicts the properties of blended aggregates so that the user can determine the necessary blending ratio to control such troublesome properties as thermal coefficient of expansion and drying shrinkage.

17. Key Words Aggregates, aggregate blends, portland cement concrete pavements, chemical modeling, aggregate properties, CHEM2 Program	18. Distribution Statement No restrictions. This document is available to the public through the National Technical Information Service, Springfield, Virginia 22161.

19. Security Classif. (of this report) Unclassified	20. Security Classif. (of this page) Unclassified	21. No. of Pages 85	22. Price

Form DOT F 1700.7 (8-72) Reproduction of completed page authorized

EFFECTS OF AGGREGATE BLENDS ON THE PROPERTIES OF PORTLAND CEMENT CONCRETE PAVEMENTS

by

Terry Dossey
B. F. McCullough
Abigail Dumas

Research Report 1244-8

Research Project 0-1244
Evaluation of the Performance of Texas Pavements Made with Different Coarse Aggregates

conducted for the

Texas Department of Transportation

in cooperation with the

U.S. Department of Transportation
Federal Highway Administration

by the

CENTER FOR TRANSPORTATION RESEARCH
Bureau of Engineering Research
THE UNIVERSITY OF TEXAS AT AUSTIN

August 1994

IMPLEMENTATION STATEMENT

The methodology, models, and computer program presented in this report may be used to estimate the performance of blended aggregates prior to the casting of concrete test specimens. The laboratory testing documented in this report demonstrates conclusively that the material properties of blended aggregate concrete, including tensile strength, compressive strength, modulus of elasticity, drying shrinkage, and thermal coefficient of expansion, may be estimated as a simple weighted average of the properties of the unblended constituents.

As documented by earlier reports in this project, summer morning placement of a high thermal coefficient concrete often leads to excessive cracking and early-age failures. Using the CHEM2 computer program, the pavement designer can determine the necessary blending ratio to mitigate such problems. Combined with the other tools developed in this project (e.g., the CRCP analysis programs), aggregate blending and steel reinforcement design can be optimized to obtain equal performance from different aggregates under a wide range of placement conditions.

Prepared in cooperation with the Texas Department of Transportation and the
U.S. Department of Transportation, Federal Highway Administration.

DISCLAIMERS

B. F. McCullough, P.E. (Texas No. 19914)
Research Supervisor

TABLE OF CONTENTS

SUMMARY

Despite recent studies that show pavement performance does vary according to the aggregate type used, current portland cement concrete pavement design tools do not fully account for such aggregate property variables in their design process. The aggregate characteristics that have been shown to affect pavement performance include strength, thermal properties, and shrinkage properties.

Thus, the objective of this study is to investigate the material properties of crushed limestone and siliceous river gravel — two aggregates predominantly used in current pavement construction — and to determine the relationship between the properties of single-aggregate concrete and concrete made with predetermined blends of limestone and gravel. This report continues the work of Project 422/1244, which was limited to single-aggregate concretes. Additional models were developed to predict concrete properties of blended aggregate concrete for use in the design tools CRCP and JRCP described in previous 422/1244 reports. A computer program, CHEM2, was developed to allow the pavement designer to identify the material properties of concrete using an inexpensive chemical test. CHEM2 also predicts the properties of blended aggregates so that the user can determine the necessary blending ratio to control such troublesome properties as thermal coefficient of expansion and drying shrinkage.

CHAPTER 1. INTRODUCTION

BACKGROUND

Aggregate technology has been growing rapidly in recent years. Reflecting the importance of aggregates in portland cement concrete, this growing technology has, for the most part, been an effort to determine how an aggregate reacts to different stresses — a determination that pavement engineers say will provide significant insight into the performance of portland cement concrete pavements constructed with various aggregate types (Ref 1). For example, under a given set of environmental conditions, changes in concrete volume stresses will vary significantly among pavements, depending on the concrete's modulus of elasticity (E), coefficient of thermal expansion (α_c), and drying shrinkage (Z). In turn, these properties (and the extent of the changes they effect) will depend largely on the materials contained within the concrete. Thus, with aggregates comprising 75 to 80 percent of that concrete's weight (and 60 to 75 percent of its volume), and given that each aggregate source is unique in its physical, chemical, and mechanical properties, there is a need for pavement engineers to consider carefully the aggregate selected for a given concrete mix design (Ref 2). In short, engineers require a method that ensures the pavements they produce will have consistent quality, regardless of the aggregate or blend of aggregates used.

There are countless sources of aggregates available in the United States. In 1989, Texas alone produced 65,226.6 kg (71.9 tons) of crushed stone, making it the nation's third largest producer of aggregates for that year (Ref 3). Within Texas, the type of the aggregate readily available for construction varies regionally. As shown in Figure 1.1, aggregate types found in Texas can vary from siliceous river gravel in Victoria (eastern Texas), to trap rock in Brownsville (south Texas), to dolomite in El Paso (western Texas), and to limestone in Georgetown (central Texas). Other aggregate types found less commonly across the state include granite, basalt, sandstone, and traprock. Of all the aggregate types, however, crushed limestone and siliceous river gravel are the two most common aggregates used in Texas for mixes of portland cement concrete.

Recent field experience has shown that aggregate type is one of the major determinants of pavement quality (Ref 4). The difference between limestones and river gravels became apparent when field surveys demonstrated that continuously reinforced concrete (CRC) pavements made with crushed limestone out-perform pavements of similar age and traffic histories made with siliceous river gravels. In an effort to utilize all available aggregate sources, researchers have begun to investigate alternative design solutions, taking into consideration various aggregate sources that could consistently produce quality pavements (Ref 5).

Previous work in this study formulated a design standard for CRC pavement wherein the longitudinal steel percentage was varied depending on the coarse aggregate type. Because the standard was developed using theoretical models, the next step was to conduct testing to verify the empirical models. Phase I testing was limited to laboratory testing and model development, with such efforts focused on a study of typical properties of concrete pavements made with either crushed limestone or river gravel. An experiment was designed to include laboratory curing conditions encompassing a variety of humidities and temperatures. The design factorial for the Phase I experiment is shown in Figure 1.2.

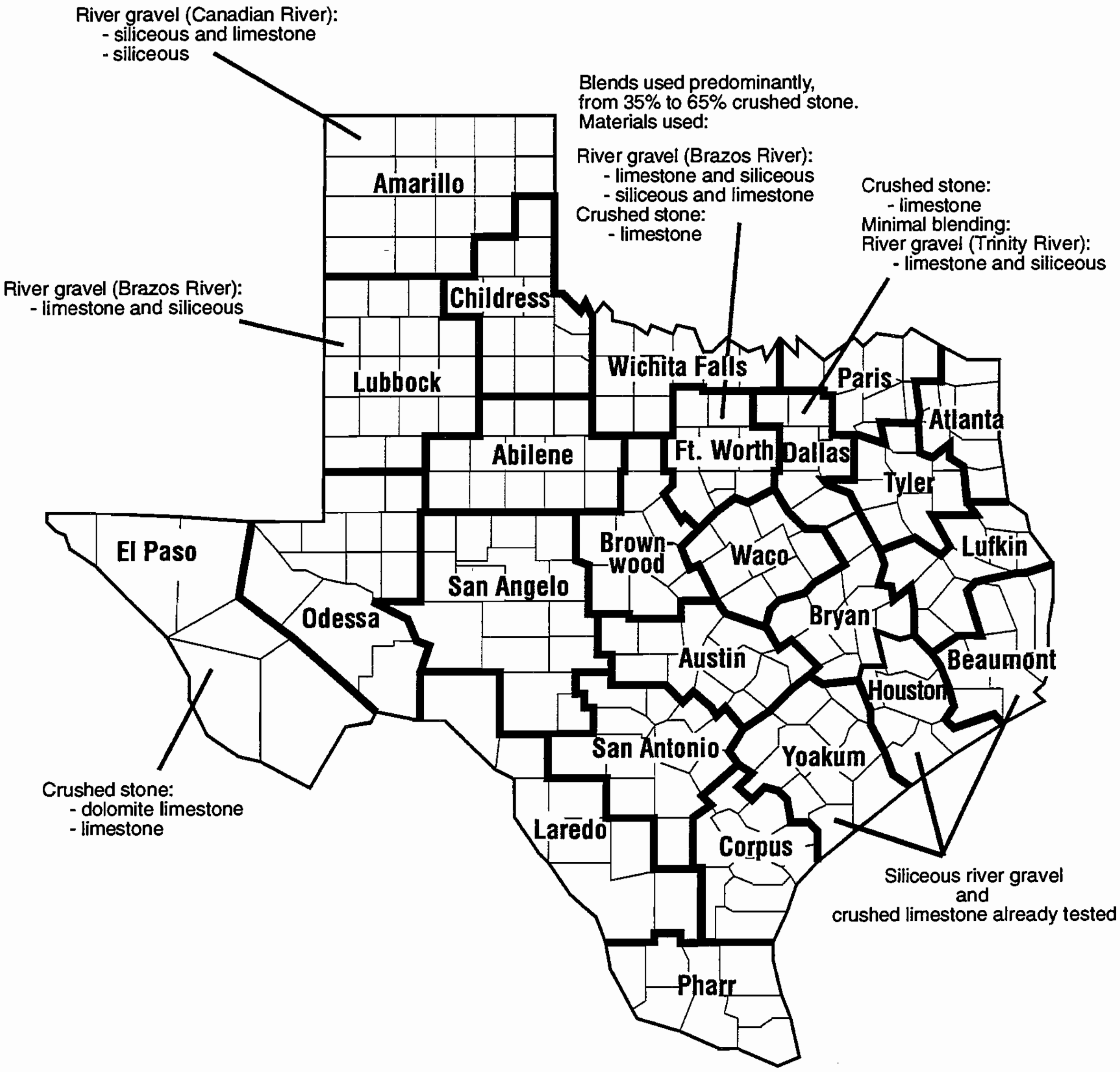

Figure 1.1 Coarse aggregates used in concrete pavements in Texas

Coarse Aggregate Types		Curing Times (days)	Moisture Conditions					
			40% Rel Humidity			100% Rel Humidity		
			Curing Temperatures					
			50°F	75°F	100°	50°F	75°F	100°
	Siliceous River	1						
		3						
		7						
		28						
		90						
	Limestone	1						
		3						
		7						
		28						
		90						

$^{\circ}C = {}^{5}/_{9}(^{\circ}F-32)$

Figure 1.2 Factorial for Phase I laboratory testing

The testing of specimens included the same four concrete properties used to develop the mechanistic design model for portland cement concrete pavements. These properties are: compressive strength (f_c), splitting tensile strength (f_t), elastic modulus (E), and drying shrinkage (Z). The results of the tests, part of the Phase I studies, were evaluated using the CRCP-4 computer program, which used the mechanistic models to study the performance measures (crack spacing, crack width, and steel stress) of pavements using these materials (Ref 2). Testing was continued to allow for the use of aggregate types other than limestone and river gravel. Phase II expanded the testing to include the six other Texas coarse aggregates shown in Table 1.1.

Table 1.1 Texas coarse aggregates used in Phase II testing

Aggregate	**Source**	**TxDOT District**	**County**
SRG	Fordyce Gravel/Chipley Pit	13	Victoria
LS	Texas Crushed Stone/Feld Pit	14	Williamson
VG	Vega Sand and Gravel/Tom Green Pit	4	Oldham
WT	Western Sand and Gravel/Tascosa Pit	4	Oldham
FR	Texas Industries/Ferris Plant	2	Parker
DL	El Paso Sand Products/McKelligon Canyon	24	El Paso
GR	TXTX Aggregates/Scotland		
BTT	50/50 blend of Texas Industries/Bridgeport and	2	Wise
	Texas Industries/Tin Top Plant # 539	2	Parker

With the new data, we developed two sets of mathematical models. The first were descriptive models (Equations 1.1 and 1.2 below) designed to characterize time-dependent properties for each of the tested aggregates. In an effort to avoid expensive and time-consuming laboratory testing, we developed models for estimating concrete properties directly from the chemical composition of the aggregate. These models, shown in Equations 1.3–1.6, permit a rough comparison of aggregates prior to laboratory testing (Ref 7).

$$F_N(t) = N_{28}(2-e^{-BT}-e^{-CT}) \qquad \text{(Eq. 1.1)}$$

$$Z_N(t) = N_{256}(2-e^{-BT}-e^{-CT}) \qquad \text{(Eq. 1.2)}$$

where:

t = the time of curing (days),

$F_N(t)$ = the normalized concrete property (f_t, f_c, or E) at time t,

$Z_N(t)$ = the normalized drying shrinkage at time t, and

N_{28}, N_{256}, B,C = coefficients of curvature specific to each aggregate given in Table 1.2

$$f_t(28) = 59.238 \bullet \ln(CaO)+46.884 \bullet \ln(MgO)+1.7159CaO/MgO+572.2 \qquad \text{(Eq. 1.3)}$$

$$f_c(28) = -403.2 \bullet \ln(CaO)+6.806CaO/Al_2O_3+5120.5 \qquad \text{(Eq. 1.4)}$$

$$E(28) = -0.4135 \bullet \ln(Al_2O_3)+0.264 \bullet \ln(MgO)-0.00948CaO/Al_2O_3+4.664 \qquad \text{(Eq. 1.5)}$$

$$Z(256) = 1.8723(CaO \bullet Al_2O_3)+0.1223CaO/Fe_2O_3-0.1383(CaO \bullet MgO)+350.6 \qquad \text{(Eq. 1.6)}$$

Table 1.2 Coefficients for Equations 1.1 and 1.2

		GR	**DL**	**VG**	**BTT**	**WT**	**FR**	**LS**	**SRG**
Compressive Strength (f_c)	A	2570.8	2236.7	1995.3	2038.2	2068.5	2000.1	2550.57	2445.25
	B	0.096	0.231	0.367	0.582	0.214	0.206	0.115	0.182
	C	0.623	0.562	0.367	0.220	0.647	0.801	0.490	0.473
	N_{28}	0.5176	0.5009	0.4978	0.4980	0.4998	0.5014	0.5102	0.5020
Tensile Strength (f_t)	A	266.46	247.06	221.08	221.85	216.01	241.94	217.83	231.07
	B	0.15	0.261	0.302	0.332	0.198	0.137	0.177	0.267
	C	1.05	1.094	0.3014	0.723	2.505	2.479	1.068	0.468
	N_{28}	0.504	0.500	0.500	0.500	0.501	0.505	0.502	0.500
Elastic Modulus (E)	A	1.678	2.324	1.882	1.992	1.803	1.979	1.802	2.282
	B	0.78	0.485	0.301	0.688	0.405	0.738	0.535	0.574
	C	1.65E14	3.537	1.574	2.00	97.056	2.668E12	110.46	61,755.1
	N_{28}	0.500	0.500	0.500	0.500	0.500	0.500	0.500	0.500
Drying Shrinkage (Z)	A	321.23	252.06	235.19	343.62	358.456	327.23	229.1	198.39
	B	0.0851	0.04062	0.3948	0.0328	0.3109	0.0745	0.0398	0.0619
	C	0.001	0.00155	0.01255	0.00069	0.000715	0.00119	0.00754	0.005
	N_{28}	0.8112	0.7569	0.5146	0.8582	0.8600	0.7828	0.5403	0.5636

The above equations present only a few examples of the models developed during Phase II. Other models were developed to predict properties at times other than 28 days, with each model type having its own specific uses and limitations. For example, the time-dependent models, while fairly accurate, are only directly applicable to the eight aggregates tested in the study. For non-tested aggregates, the chemical models can be used for estimates of properties, though additional care must be taken to remain within the inference space of the models. A user-friendly computer program, CHEM, has been developed for use in applying the chemical models. The program requests percentage by weight of four key chemical components, which can be obtained from an inexpensive chemical analysis of the aggregate. The program then creates predicted curing curves for tensile strength, compressive strength, elastic modulus, and drying shrinkage (Ref 7).

Phases I and II verified the importance of the relationship between coarse aggregate type and portland cement concrete properties. With this knowledge, we continued the study by focusing on two predominant coarse aggregate types: crushed limestone and siliceous river gravel. The new testing, Phase III, will clarify the necessity of incorporating aggregate type into the design process by increasing the data available for evaluation and by providing a new basis for the study of aggregate blending and its affects on pavement properties.

OBJECTIVES

Currently, the effects of aggregate type can be accurately assessed only by casting cylinders and conducting destructive tests in the laboratory to determine variation in concrete properties. If the mix design is held constant — the only change being the type of coarse aggregate used — any resulting differences in tested properties could be attributed to the aggregate or to normal material variability. (This being true only if the volume of coarse aggregate remains equal, while the weight would change in accordance to varying specific gravity.) This was the same methodology used in Phase II testing.

Phase III of this study, discussed in this report, will increase our understanding of aggregate properties and their relationship to pavement properties. Through an intensive laboratory study, concretes made with blends of crushed limestone and siliceous river gravel were compared with concretes constituted of single aggregate types. The resulting lab data will be used to verify and support the following assumptions:

- Concrete pavements constructed with a blend of aggregates will have properties that vary in proportion to the amount of each aggregate type, or types, used in the mix.
- Portland cement concrete can be designed to adapt to any coarse aggregate type and still produce quality pavements by using aggregate blends effectively.

With the increased volume of data, existing mathematical models relating mineralogical oxides of the aggregates to some of their properties developed in Phase II can be refined for use as a design tool. Models relating properties to aggregate blends and types will be created to help develop a selection process for appropriate blends. An additional objective to be completed will be the inclusion of aggregate blends in the existing computer pavement design and analysis program, CRCP.

SCOPE

In addition to the four properties tested in Phases I, II, and III (f_c, f_t, E, Z, α_c), a number of other factors affect concrete pavement performance, including proper grading, maximum aggregate size, and surface texture. These considerations, while discussed briefly in this report, remain outside the scope of this study. All aggregates used were properly sized and graded for the tested mix design.

With respect to report organization, Chapter 2 of this report will review aggregate properties and their role in producing a quality portland cement concrete (PCC) pavement. Chapter 3 considers the specific chemical, mechanical, and physical properties of an ideal aggregate. It also lays out concepts for categorizing concrete coarse aggregates. Chapter 4 discusses the laboratory experiment of Phase III conducted to support the feasibility of blended aggregate mixes. Chapter 5 analyzes the laboratory data through statistical regression analysis and through comparison with Phase I and II results. Chapter 6 reviews the implementation possibilities for the results of this project and presents ideas for future development. The final chapter, Chapter 7, explains the significance of this study and suggests further areas of study.

CHAPTER 2. CURRENT AGGREGATE TECHNOLOGY

ASTM C 294 provides a basic method for categorizing mineral aggregates into three major divisions: igneous, sedimentary, and metamorphic. Each of these groups is then further divided into subcategories according to mineral and chemical composition, texture, and internal structure. While these descriptions are useful, there are many more factors to consider when deciding on the quality of a coarse aggregate. A more thorough description of an aggregate type would have to include physical and mechanical attributes, as well as chemical composition and mineralogy. Physical properties define an aggregate particle in terms of length, time, and mass. Mechanical properties, which are behavioral properties, identify a particle's physical reaction to an externally applied force. Chemical properties identify an aggregate particle chemically and/or indicate the changes the particle undergoes as a result of a chemical process (Ref 3). All of the individual properties in each of these areas are defined in Appendix A.

To be considered appropriate for use in a PCC pavement, an aggregate does not have to exhibit ideal properties in all areas. Each project must be considered separately to determine which properties are of greater importance in an aggregate. The National Stone Association's *Aggregate Handbook* (Ref 3) provides a table showing "properties that an aggregate must possess so that the system fulfills its function" (Table 2.1).

PHYSICAL PROPERTIES

An aggregate's physical properties affect a pavement in a number of ways, including workability, finishability, traffic load capacity, and other construction- and performance-related areas. Some contributing aggregate physical properties include:

- particle shape
- maximum particle size
- surface texture
- percent voids
- thermal conductivity
- permeability
- specific gravity
- porosity
- VMA
- gradation

During construction, these physical properties determine how the aggregate particles will mix with each other and the cement paste, and how well the mix will set around steel reinforcement (Ref

12). Using these properties to compare limestone and river gravel reveals their significant differences. Crushed limestone is angular and rough, while siliceous river gravels are rounded and smooth. On the one hand, such smoothness makes the river gravel easier to work with; on the other hand, this property decreases the aggregate's ability to bond with the cement paste. When bond strength is decreased, the concrete strength is reduced accordingly, perhaps affecting at the same time the mix water/cement ratio and sand volume (Ref 10). Conversely, a coarse aggregate with high angularity is difficult to mix. For adequate workability, the mix would require more sand to provide lubrication for the larger aggregate — a requirement that increases the surface area (i.e., the sand) and, therefore, the amount of water needed in the mix, affecting the water/cement ratio. Smooth aggregates, which roll easily over each other, do not need the extra sand; as a result, the mix requires a lower water/cement ratio.

Table 2.1 Aggregate properties for specific uses to meet functions of system[1]

Function	**Property**	**PCC**	**Aggregate Asph. Conc.**	**Relative Importance of Property[1] Base**
1. Adequate internal strength & stability to distribute surface pressures and to prevent extensive surface deflections	1. Mass stability	NA	I	I
	2. Particle strength	I	I	I
	3. Particle stiffness	I	I	I
	4. Particle surface texture	I	I	I
	5. Particle shape	I	I	I
	6. Grading	I	I	I
	7. Maximum particle size	I	I	I
2. Resistance to deteriorating effects of weather and chemical actions	1. Resistance to chemicals, such as salts	I	U	NA
	2. Solubility	I	I	I
	3. Slaking	I	I	I
	4. Resistance to wetting-drying	I	U	I
	5. Resistance to freezing-thawing	I	U	I
	6. Pore structure	I	I	I
3. Resistance to deteriorating effects produced by applied loads	1. Resistance to degradation	I	I	I

---

[1] I = Important; N = Not Important; U = Importance Unknown; NA = Not Applicable; PCC = portland cement concrete; Asph. Conc. = Bituminous or asphalt concrete; Base = Unbound aggregate base

Table 2.1 Continued

Function	Property	PCC	Aggregate Asph. Conc.	Relative Importance of Property[1] Base
4. Resistance to the effects of internal forces, such as expansion, contraction, warping, and curling	1. Volume change- thermal	I	N	N
	2. Volume change - wetting and drying	I	N	N
	3. Pore structure	I	N	N
	4. Thermal conductivity	I	N	U
5. Aggregate and binder compatibility	1. Chemical compounds reactivity	I	I	N
	2. Organic material reactivity	I	N	N
	3. Coatings	I	I	N
	4. Thermal volume stability	I	N	N
	5. Base exchange	I	I	I
	6. Surface charges	N	I	N
	7. Pore structure	U	N	N
6. Retention of a surface that will assure acceptable standards of performance. To have this characteristic, consider the following surface properties:				
a. Skid resistance	1. Particle shape	I	I	NA
	2. Particle surface texture	I	I	NA
	3. Maximum particle size	N	I	NA
	4. Particle strength	I	I	NA
	5. Wear resistance	I	I	NA
	6. Particle shape of abraded fragm.	I	I	NA
	7. Pore structure	I	I	NA
b. Surface roughness	1. Maximum particle size	I	I	NA
	2. Grading	I	I	NA
c. Glare and light reflection	1. Reflection	I	I	NA
	2. Glare	I	I	NA
d. Loose material	1. Resist. to degradation	I	I	NA
	2. Specific gravity	N	N	NA
e. Tire wear	1. Particle shape	I	I	NA
	2. Particle surface texture	I	I	NA
	3. Maximum particle size	I	I	NA
f. Rolling resistance	1. Maximum particle size	U	I	NA
	2. Particle shape	I	I	NA

[1] I = Important; N = Not Important; U = Importance Unknown; NA = Not Applicable; PCC = portland cement concrete; Asph. Conc. = Bituminous or asphalt concrete; Base = Unbound aggregate base

Table 2.1 Continued

Function	Property	PCC	Aggregate Asph. Conc.	Relative Importance of Property[1] Base
g. Noise level	1. Maximum particle size	U	I	NA
h. Electrostatic properties	1. Electrical conductivity	U	I	NA
i. Appearance	1. Particle color	N	N	NA
	2. Oxidation and hydration reactivity (stains and popouts)	I	N	NA
7. Retention of prop. during the construction process that supports all other functions of the system	1. Maximum particle size	I	I	I
	2. Resistance to degradation	I	I	I
	3. Integrity during heating	N	I	N

[1] I = Important; N = Not Important; U = Importance Unknown; NA = Not Applicable; PCC = portland cement concrete; Asph. Conc. = Bituminous or asphalt concrete; Base = Unbound aggregate base

Strength and durability of a finished pavement are also affected by physical properties. Both compressive and tensile strength will typically be lessened with an increase in the water/cement ratio. Strength can also be affected by the aggregate's shape: During compressive strength tests, a cylinder is more likely to crack *around* a smooth aggregate, whereas it will crack *through* an angular aggregate. This suggests that a smooth aggregate is not providing its full strength potential to the concrete because of low bonding at the aggregate/cement interface. The durability of a pavement is affected by the aggregates' ability to hold water within the particles themselves and within the voids between the aggregates. Expansion of the water in these voids owing to thermal changes can cause microcracking and popouts at the pavement surface. Porosity of an aggregate particle is determined by the aggregate composition, for example, whether it is crystalline or plate-like. An aggregate having high porosity, produced by impermeable, non-interconnected pore spaces, is generally superior to aggregate having permeable pore spaces; accordingly, they are preferred for most construction applications. Permeability is considered high if a group of aggregate particles have a large percentage of interconnected pore spaces that allow water to expand. The overall permeability of a group of particles is determined by grading and density of a mixture of aggregate particles.

MECHANICAL PROPERTIES

The mechanical properties of a coarse aggregate are behavioral — meaning they show how an aggregate reacts to such external forces as wheel loads, construction loads, and other stresses. Examples of these properties include:

- strength,
- elastic modulus,

- coefficient of thermal expansion,
- resilient modulus,
- resistance to loads, and
- resistance to degradation.

These properties pertain to hardened concrete. Strength requirements are typically easily met, being a function of aggregate grading, cement and aggregate quality, and mix design. However, designing pavements to have the other properties in acceptable ranges is not a simple task. Material interaction and environmental effects play a key role in developing desirable properties in hardened concrete. The thermal characteristics of an aggregate particle will heavily influence the extent of cracking, curling, and other temperature-related distresses. Studies have shown that placing concrete so that the heat of hydration peak does not coincide with the peak heat of the day allows the use of aggregates with higher thermal coefficients, as shown in Figure 2.1 (Ref 9). With proper consideration of these characteristics, it should be possible to use marginal aggregates effectively.

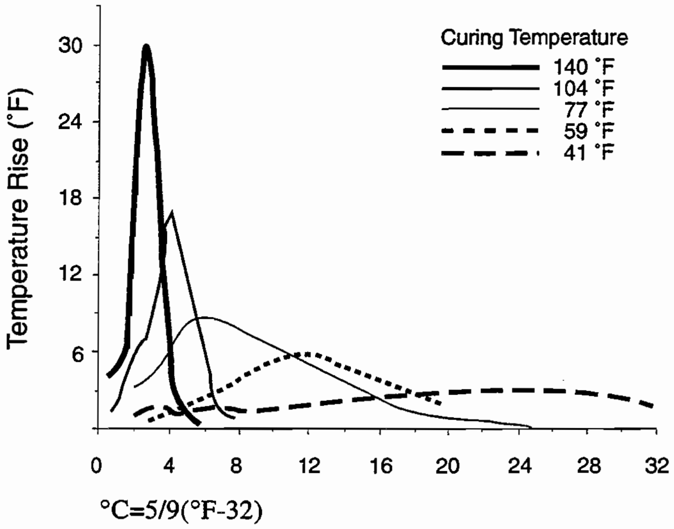

Figure 2.1 Effect of placement temperature on concrete heat of hydration (from Ref 9).

CHEMICAL PROPERTIES

At present, the chemical properties of an aggregate are considered only to prevent incompatibility with the binder and serious deterioration of the aggregate particles. Most chemical problems are due to such external sources as de-icing salts (or other water-born reactive substances) and warm, moist environments that promote internal reactions. These properties include: (1) solubility; (2) base exchange; (3) surface charge; (4) chloride content; (5) reactivity; (6) slaking; (7) coatings; (8) oxidation potential; and (9) resistivity.

Many chemical problems involve water sources. Aggregate solubility, for example, is affected by the level of acidity in mix water, runoff water, and other sources that frequently douse pavements. This same water can produce slaking, coating, and increased oxidation potential. Aggregate mineralogy will be a key source of understanding chemical properties when more is understood about its relation to pavement properties.

QUALITY MANAGEMENT

The Texas Department of Transportation's Materials and Tests Division currently operates an Aggregate Quality Monitoring Program (AQMP) to monitor TxDOT aggregate producers. To be on the approved list, an aggregate producer must regularly allow a sampling from normal production to be tested in TxDOT labs. The sample is run through three tests (Ref 1): "Abrasion of Coarse Aggregate by Use of the Los Angeles Machine" (TEX-410-A), "Soundness of Aggregate by use of Sodium Sulfate or Magnesium Sulfate" (TEX-411-A), and "Accelerated Polish Test for Coarse Aggregate" (TEX-438-A). These tests are described in the *1987 Manual of Testing Procedures — Physical Section, SDHPT 400-A Series* (Ref 11). The LA. Abrasion Test, similar to ASTM C 131, is used as a preliminary procedure for estimating aggregate soundness in terms of percent loss during a test cycle. The Soundness Test conducted by TxDOT is a modified version of ASTM C 88. It is also measured in percent loss. Compared with the impact resistance in the LA. Abrasion Test, this test measures resistance to disintegration by saturated solutions of magnesium sulfate or sodium sulfate. The Accelerated Polish Test provides a relative measure of the extent to which a pavement surface polishes under traffic. The method used is a modification of ASTM D 3319 and E 303 (Ref 11).

The programs described above seek to eliminate the use of poor quality aggregates in construction. By narrowing the selection field, pavement designers will be able to incorporate more detailed aggregate selection processes into the design phase of a pavement without increasing the amount of time and effort. Further aggregate selection techniques will be developed from this research project to assist the design expert even further.

SUMMARY

Current aggregate technology is moving towards a design process that will incorporate aggregate properties. With an increase in aggregate monitoring, it will be possible to produce pavements that meet performance specifications with readily available aggregates, which might be of poor or marginal quality, by blending with a higher quality aggregate. By understanding the relationship between blends and pure aggregate concretes, it will be possible to limit the increase in costs resulting from the higher, less available aggregate.

CHAPTER 3. AGGREGATE CHARACTERISTICS FOR DESIRED PAVEMENT PERFORMANCE

In the construction of portland cement concrete pavements, the contractor customarily selects the coarse aggregate for the project based on availability, cost, and usability. A contractor, knowing from experience what materials are easier to work with, will select the one which is familiar to him or her. While this is a valid decision process, it does not consider all of an aggregate's attributes. The aggregate's properties need to be included in the deciding factors for selection. With the number of properties to consider, it would be difficult for all of them to be incorporated individually into a decision process. From the discussion in Chapter 2, it is possible to select a small number of primary properties.

PERFORMANCE MEASURES

When a pavement is judged after completion, the performance is discussed in terms of crack spacing, crack width, steel stress, and other measurable quantities. Therefore, when discussing an aggregate, it is realistic to consider it in these terms as well. An aggregate has properties, as shown in Chapter 2, that affect pavement performance. Bond strength between the aggregate and binder, expansion characteristics of the aggregate and pavement composition, and reactivity of the aggregate will all be controlling factors in producing stresses that affect these measures. The various properties that affect these attributes are discussed below.

The strength of the bond between aggregate particles and the portland cement binder increases with the angularity of the aggregate particles, going from low bond strength with smooth and rounded aggregates, to a higher bond strength with rough and angular aggregates. A relative measure of bond strength is ASTM C496 Splitting Tension Test (Fig 3.1a) (Ref 14). When standard 15.24-cm (6-inch) diameter cylinders are tested, the plane of tensile failure will go around smooth, round aggregates, showing that the bond was weaker than the force, or go through rough, angular aggregates, showing that the bond was stronger than the failure force (Fig 3.1b) (Ref 12).

Stresses caused by temperature changes are directly related to the expansion characteristics and thermal properties of the pavement materials. Compatibility between aggregate and binder is essential for a quality pavement. The coefficient of thermal expansion (α_c) of an aggregate is its mineralogy. Both temperature and moisture affect the expansion of an aggregate. ASTM C-531 provides a quantitative measure of α_c when conducted in a controlled environment. Table 3.1, taken from the *Aggregate Handbook* published by the National Stone Association (Ref 3), lists typical ranges of ten properties of common aggregate.

Although a pavement with low expansion properties is desirable, field work has shown that season of placement is an important factor in controlling tensile stresses, owing to thermal changes and expansion (Fig 3.2). Thus:

> The season of placement affects pavement performance in that temperature-induced stresses will vary with time of placement, air temperature, and heat of hydration (Ref 9).

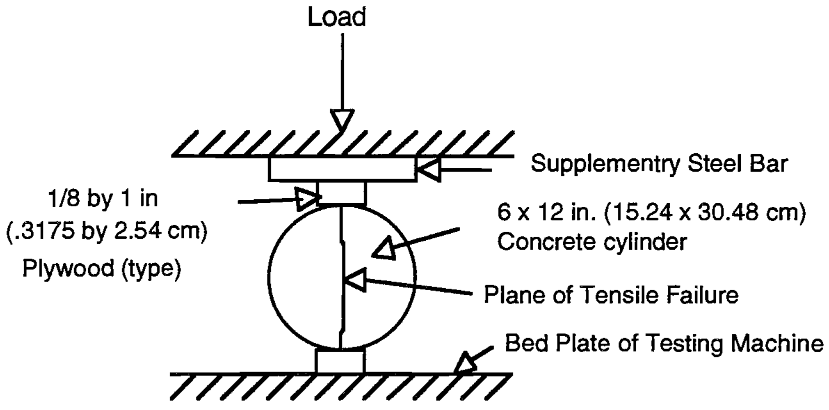

Figure 3.1a Diagrammatic arrangement of the splitting tensile test (ASTM C-496)

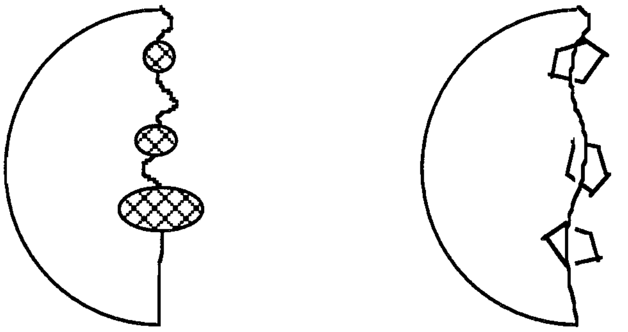

Figure 3.1b Profiles of tested concrete cylinders made with smooth, rounded aggregate, left, and angular aggregate, right

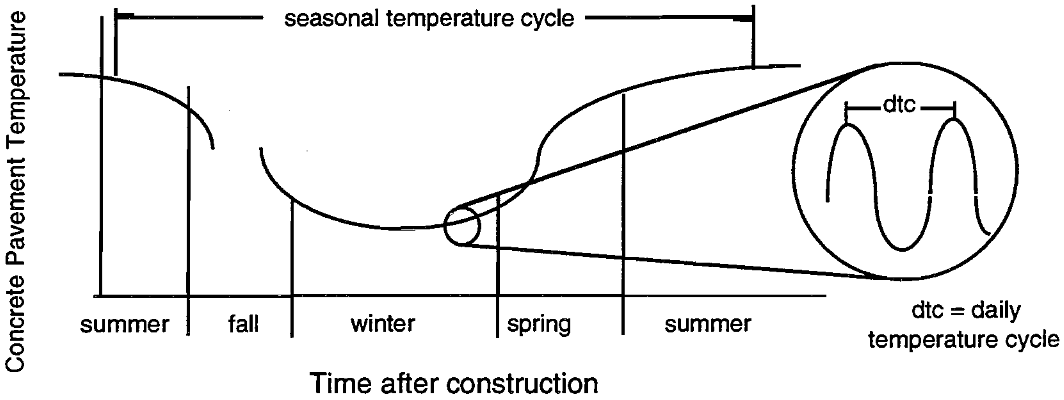

Figure 3.2 Schematic concrete pavement seasonal and daily temperature cycles

Table 3.1 Typical properties of common aggregate

Property	Granite	Limestone	Quartzite	Sandstone
1. Unit Weight (pcf)	162-172	117-175	165-170	119-168
2. Compressive Strength (x 10^3 psi)	5-67	2.6-28	16-45	5-20
3. Tensile Strength (psi)	427-711	427-853	NA (1)	142-427
4. Shear Strength (x 10^3 psi)	3.7-4.8	0.8-3.6	NA (1)	0.3-3.0
5. Modulus of Rupture (psi)	1380-5550	500-2000	NA (1)	700-2300
6. Modulus of Elasticity (x 10^6 psi)	4.5-8.7	4.3-8.1	NA (1)	2.3-10.8
7. Water Absorption (% by wt)	0.07-0.30	0.50-24.0	0.10-2.0	2.0-12.0
8. Avg. Porosity (%)	0.4-3.8	1.1-31.0	1.5-1.9	1.9-27.3
9. Linear Expansion (x 10^{-6} in./in./°C)	1.8-11.9	0.9-2.2	7.0-13.1	4.3-13.9
10. Specific Gravity	2.60-2.76	1.88-2.81	2.65-2.73	2.44-2.61

[1] NA = Data not available
psi = 6.89 kPa

A FIELD STUDY

For one field study, four test sections were constructed in Houston at two locations. At each location, one section was constructed during the summer and the other during the winter, producing varying types of temperature histories for the sections. It had been hypothesized that the time and season of placement had a large effect on performance when considered in conjunction with concrete curing temperatures. Concrete temperature history can be characterized by three periods:

(1) the concrete set temperature (which is affected by heat of hydration) at which concrete transforms from a plastic to a solid;

(2) the daily concrete temperature cycle, especially the minimum daily concrete temperature (before the concrete gains full strength); and

(3) the seasonal concrete temperature cycle, especially the minimal yearly concrete temperature (Fig 3.3)(Ref 9).

The magnitude and the rate of the heat of hydration is a function of the initial concrete placement temperature. The heat of hydration will peak higher and more quickly for a high placement temperature than for a lower placement temperature. The effect of placement temperature on heat of hydration is shown in Figure 2.1 (Refs 15, 16).

While pavement performance is generally considered in terms of space and time, it can also be well-described as a function of its material variability and its loading history. The less variability, the higher the equality of pavement performance. But as discussed in earlier chapters, aggregates are not uniform among pavements. Therefore, not all pavements will perform at equal levels. Since the aggregate type is not constant, other factors within the design must be adjusted to reduce pavement performance variability.

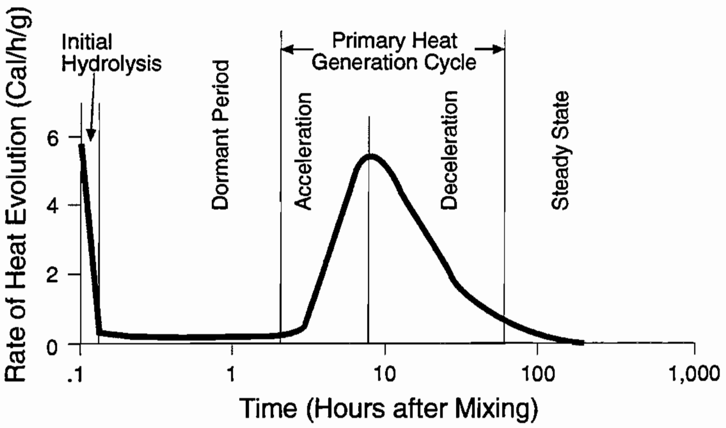

Figure 3.3 Schematic representation of the heat of hydration vs. time on concrete tricalcium silicate (Ref 18)

Judging pavement variability and quality is often more subjective than quantitative. A method of comparing pavement performance is ride quality, usually discussed in terms of the present serviceability index, or PSI. PSI can be considered a function of the distresses that affect ride quality. Earlier studies have used crack spacing, crack width, and steel stress to predict performance of a pavement. One such study, discussed earlier, conducted a survey of test sections placed around the Houston area (Fig 3.4). The variables of the study included the following:

(1) coarse aggregates (crushed limestone and siliceous river gravel),

(2) longitudinal reinforcing steel percentages (design %, +0.1%, -0.1%),

(3) available bond areas (#6 bar and #7 bar),

(4) concrete slab thickness (25.4 cm [10 in.], 27.9 cm [11 in.], and 38 cm [15 in.]); and

(5) season of placement (summer and winter).

Analyzing all possible combinations required 72 test sections. The study team measured crack spacing with a roller tape, recording at the same time each crack's location at the edge of the pavement. The difference between these measurements represented the recorded crack spacing. Crack widths were measured using a microscope having a scale of .0254 mm (0.001-inch) gradations and a resolution of x60. While steel stress was not monitored in this study, no distress was found to be associated with steel yield during the monitoring of the test sections.

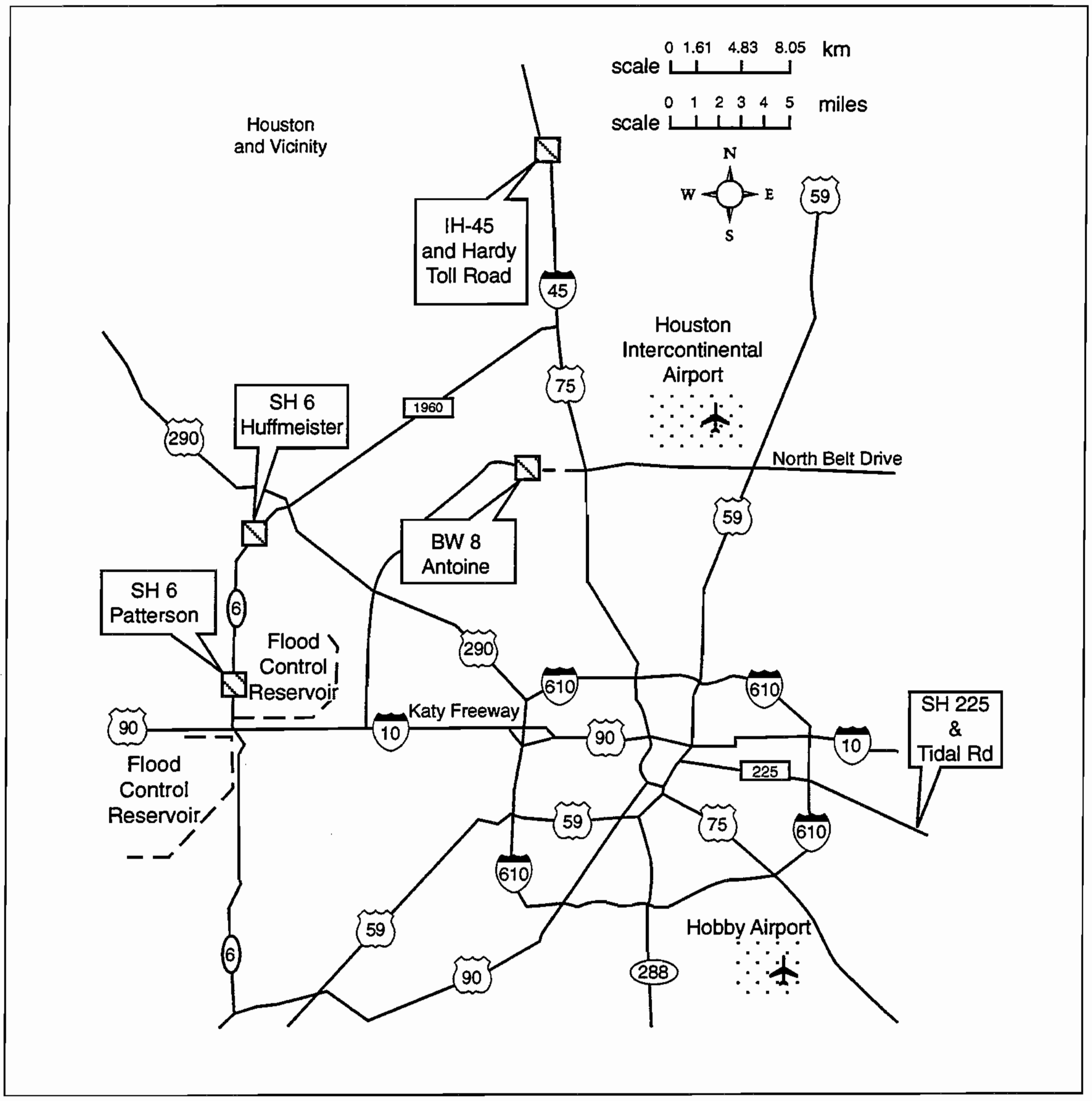

Figure 3.4 Location and season of placement of the test sections

Early observations (first 30 days after construction) concluded the following:

(1) For the paired (equivalent) test sections, there was a significant difference in crack spacing between the siliceous river gravel (SRG) and the limestone (LS) sections. The LS sections, without exception, exhibited fewer cracks and larger crack spacings than the SRG sections.

(2) Generally, with the winter projects the crack spacing decreased as the percent steel increased. At 1 month, a change in bond area achieved by the use of different bar sizes (No. 6 and No. 7 bars) did not yield a significant difference in crack spacing.

(3) The CRCP program reliably predicted crack spacing (both mean crack spacings and crack spacing distribution) occurring during early life (Ref 9).

After monitoring the test sections for 2 years, the study produced the following conclusions. The project constructed in the summer experienced crack spacing distributions with the greatest number of cracks under the 1.07-m (3.5-ft) lower limit recommended by AASHTO to minimize the probability of punchouts (Fig 3.5). The IH-45 project had a greater number of cracks at the .9144-m (3-ft) range than expected, a result of the use of reinforcing steel in two layers, which created a weak concrete plane that induced cracks over the transverse steel.

The sections with a lower steel percentage had the greater average crack spacing for most of the projects. No definite trend could be seen with respect to crack spacing and reinforcing bar diameters. The manholes in the SH 6S project caused some unusual distress in this section, resulting in some punchouts 1 year after construction. The SRG sections, though having a lower percentage of steel, showed closer average crack spacings than the LS sections.

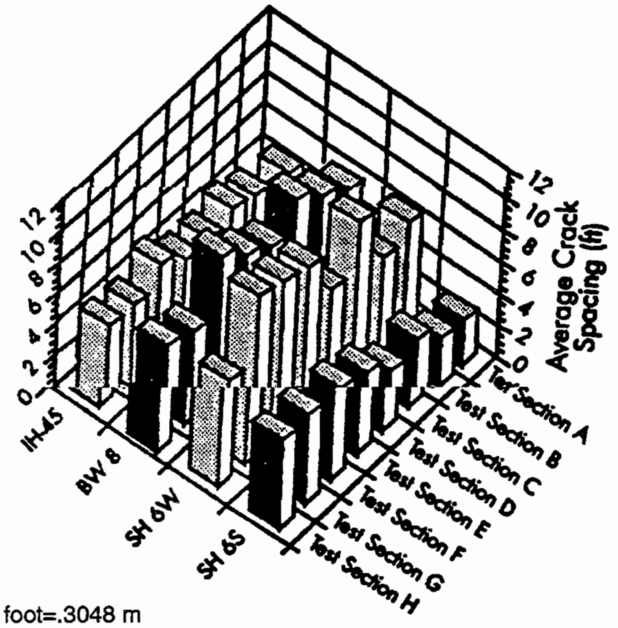

1 foot=.3048 m

Figure 3.5 Measured average crack spacing of Houston CRCP test sections by project location

The test sections placed in the summer had greater crack widths than those placed in the winter, suggesting that temperature (namely, the differential between setting temperature and seasonal temperature) plays a significant role in determining crack width (Fig 3.6). Theoretically, a higher steel percentage contributes to a smaller crack, while a larger reinforcing steel-bar diameter yields a wider crack. While this pattern was not consistent throughout all the test sections, a slight correlation could be seen.

Finally, the SRG test sections had a higher average crack width than the equivalent LS test sections. This may also be attributed to the fact that SRG coarse aggregate has a significantly higher thermal coefficient than the LS coarse aggregate.

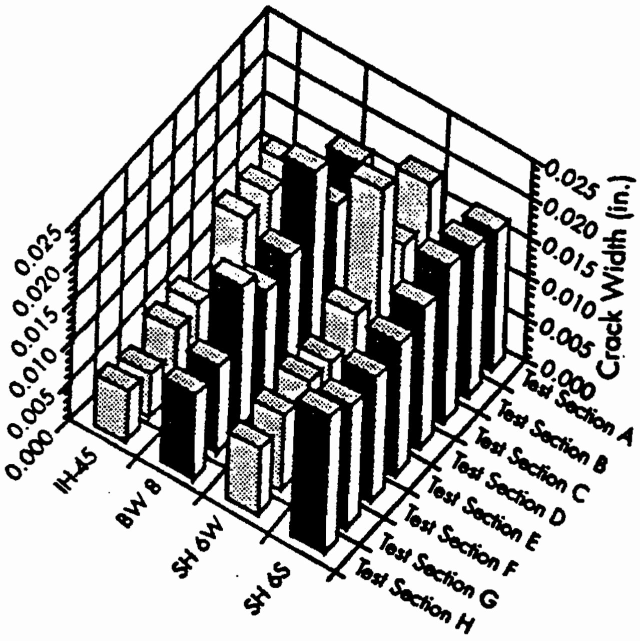

1 inch=2.54 cm

Figure 3.6 Measured average crack width of Houston CRCP test sections by project location

COMPUTER DESIGN TOOLS

The CRCP-7 program, a mechanistic model developed at the Center for Transportation Research of The University of Texas at Austin, predicts CRCP performance and behavior as a function of crack spacing, crack width, steel stress, and number of punchouts per lane per ESAL (80 kN, or 18-kip, equivalent single axle loads). This program was evaluated using crack spacing and crack width field data collected during the previously discussed research project. It provided a good fit for average crack spacings, but a poor fit for crack distribution, because it assumes a normal distribution while, in reality, the test sections show a bimodal crack spacing distribution. For crack widths, it was found that crack width and crack spacing do not necessarily correlate; the factors having the greatest impact on crack width were found to be the day of crack occurrence, residual shrinkage, reinforcing steel percent, area of bond contact, and elastic modulus of the concrete.

Through this and other research projects, the CRCP-7 program has been refined and improved. In the current study, we plan to incorporate aggregate composition and aggregate blends as additional prediction factors in the CRCP-7 program. This will allow for consideration of various aggregate types and blends in the prediction of properties prior to lab testing. The first step towards this revision will be the development of CHEM2, a chemical analysis program also designed by CTR. The initial CHEM1 program was developed from the Phase I and II testing of eight Texas aggregates. This program requires as input the percentages by weight of certain oxide residues produced by standard fusion testing. It then outputs graphs predicting f_t, f_c, E, and Z for curing times ranging from 1 to 28 (256 for Z) days. Phase III will provide additional data to enhance predictive ability for limestones and siliceous river gravels. It will also provide the basis for the development of blended aggregate prediction models. The CRCP-7 program will be modified to allow the input of the values produced by CHEM2 to give performance predictions for pavements constructed with those aggregates or blends. Eventually, the final CRCP program should be a helpful design tool by providing a means of incorporating aggregate type. It will also eliminate time-consuming lab testing by providing a means of evaluating different aggregate options prior to mix design.

An aggregate categorization method would be a useful development for accurate selection of aggregate types suitable for a projects needs. A conceptual method for categorizing aggregates is shown in Figure 3.7. It considers factors needed for selection in a general sense only. Further development is necessary before this is a viable tool. It should be assumed by the designer using this method that any chosen aggregate would be used with proper gradation.

The first step for this method of categorization of an aggregate is to conduct a chemical analysis of the sample. This will provide insight into the composition and, hence, the source of the aggregate. From the composition group, the next division will be into property groups. Each property can be considered separately, such as the four discussed in this report (i.e., compressive strength, tensile strength, elastic modulus, and thermal expansion). Each composition group will have a range of expected values for a property. Examples of these ranges are shown in Table 3.1 (Ref 3). Using identity labels for composition group and property groups and ranges, a category code can be used that would make it easy to recognize quickly an aggregate's quality for use in a project.

Aggregate selection can be based on many factors. Developing design tools to allow for quick selection of an aggregate type or blend will increase the quality and life span of a portland cement concrete pavement. Both aggregate property values and the relationship they have with pavement performance should be added into the basic design of a pavement.

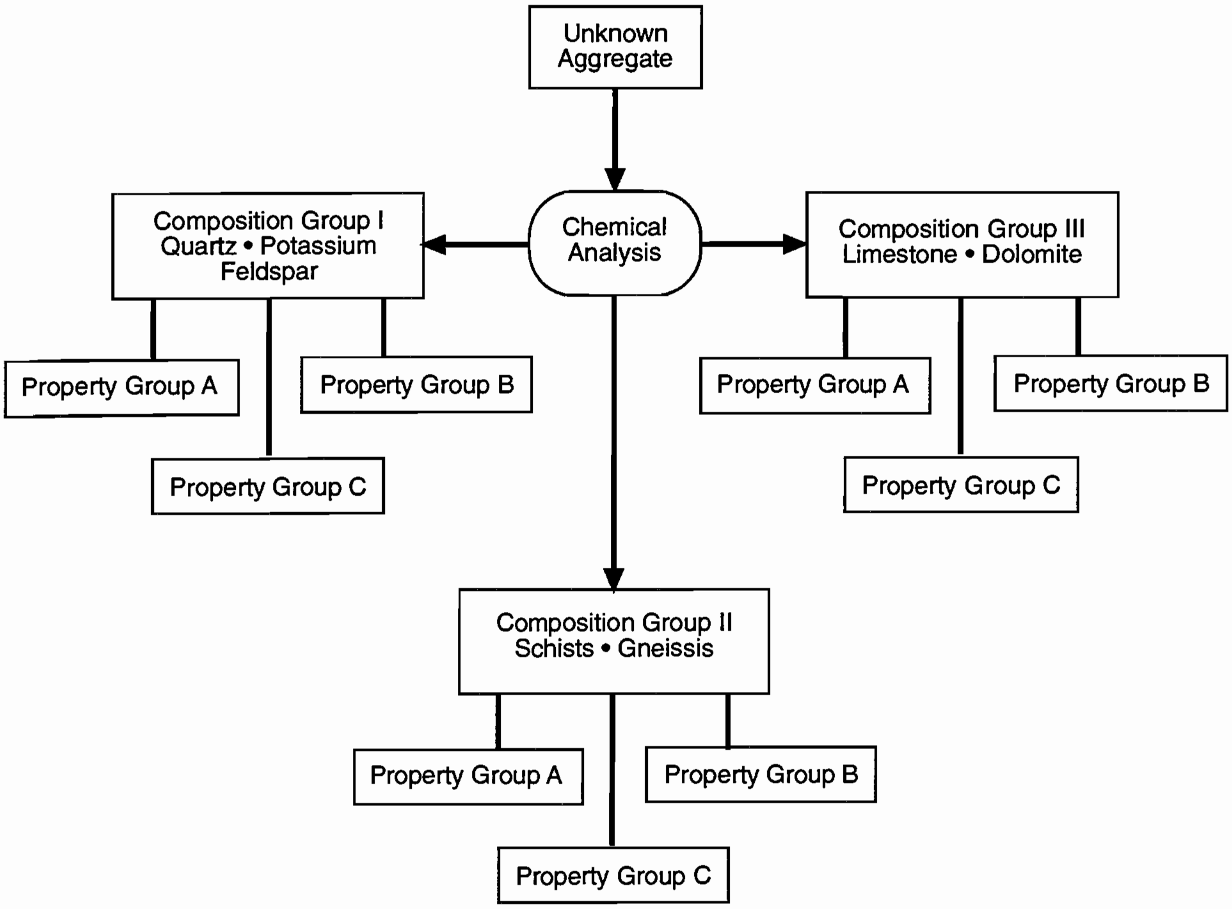

Figure 3.7 Flowchart for conceptual categorization

CHAPTER 4. THE LAB WORK

Given the variety of aggregates available for concrete pavement construction, pavement designers require a quick and easy method for selecting an aggregate that meets the needs of a particular project. By using a categorization technique for coarse aggregates (as discussed in Chapter 3), a pavement designer could select an aggregate quickly by looking only at the properties and characteristics that are most important to the project.

Concrete behavior is readily predictable for concrete made with a single type of aggregate. However, a singular aggregate type does not always provide the desired properties for every project. An alternative is a controlled blending of two aggregate types to promote desired properties (and to diminish the less desirable ones). Presently, when using controlled blending of two different aggregate types, there is no method for prediction of pavement properties. The relationship between pure aggregate concrete and blended aggregate concrete is thought to be linear, as shown in Figure 4.1, for a number of concrete properties. This study seeks to verify that concept through laboratory research and field analysis of test pavements.

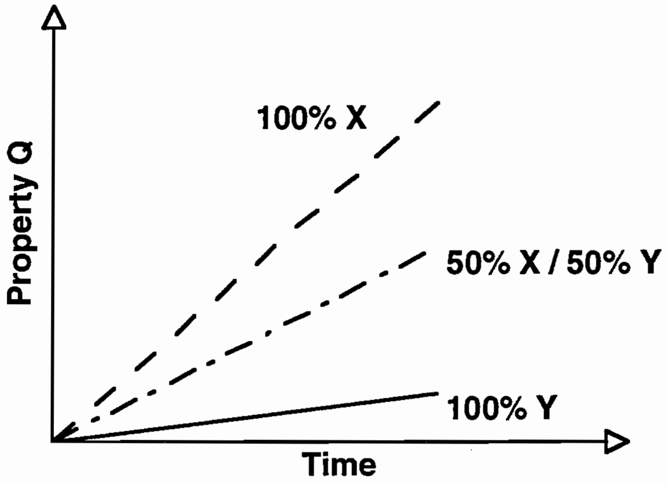

Figure 4.1 Conceptual relationship of pure and blended aggregate concretes

TESTING PLAN

While every pavement has a need for compressive and tensile strength, other factors have shown to be of equal importance, including coefficient of thermal expansion and elastic modulus (Ref 9). To determine how all of these properties vary between types of aggregates and their blends, we conducted the following laboratory study.

Concentrating on the four above named properties, the experiment was designed to support the concept of the linear relationship between singular aggregate concretes and blended aggregate concretes. For each test group, mixes using blends of two aggregates were designed, keeping all material quantities constant except the volumes of the coarse aggregate. (Weights of the coarse aggregate varied owing to different specific gravities.) Fine aggregate type was held constant throughout the experiment. From each mix, twenty-four 15.24-cm (6-inch) diameter cylinders were cast along with three 10.16-cm-by-10.16-cm-by-30.48 cm (4-inch-by-4-inch-by-12-inch) bars. The following testing program was developed.

Mix	% Limestone	% River Gravel
1, 6 & 7	100	0
2 & 8	67	33
3	50	50
4 & 9	33	67
5 & 10	0	100

Mix 1 resulted in very poor quality specimens. It was repeated as Mix 6 after the first six mixes were made and testing had begun. The linearity became apparent so the number of mixes was reduced, eliminating the 50/50 percent mix from the second round of testing.

TEST METHODS

The following standard testing procedures were used for the laboratory experiment. Only one test, Elastic Modulus, was modified; it was used, as in previous Phase I and II test procedures, to enable a comparison of data from all three phases.

- ASTM C 39-86 Standard Test Method for Compressive (f'_c) Strength of Cylindrical Concrete Specimens
- ASTM C 469-90 Standard Test Method for Static Modulus of Elasticity (E) and Poison's Ratio of Concrete in Compression (Modified)
- ASTM C 496-90 Standard Test Method for Splitting Tensile (f_t) Strength of Cylindrical Concrete Specimens
- ASTM C 531-90 Standard Test Method for Linear Shrinkage and (a_c) Coefficient of Thermal Expansion of Chemical-Resistant Mortars, Grouts and Monolithic Surfacings (Modified)

Three specimens were tested for each property when possible. The results showed that there is some linearity, within a property, among the blends.

MATERIAL CHARACTERIZATION

Compressive Strength (f_c)

Compressive strength was determined after 1, 3, 7, and 28 days of curing, according to ASTM C-39 (14), which consists of the application of a continuous compressive axial load to the molded concrete cylinders at a prescribed rate until failure. Table 4.1 summarizes the results. Figure 4.2 presents the relationship between the pure aggregate and blended aggregate mixes.

Tensile Strength

Tensile strength was also measured at 1, 3, 7, and 28 days using a split tensile cylinder test specified in ASTM C-496 (Ref 14). This test involves applying a load over the entire length of the specimen and then recording the maximum load indicated at failure. The tensile strength is calculated by the formula

$$f_t = \frac{2P}{\pi l d}$$

where:

f_t = splitting tensile strength (psi),

P = maximum applied load (lb),

l = length (in.), and

d = diameter (in.).

The results are given in Table 4.2 and in Figure 4.3.

Table 4.1 Compressive strength (psi)

Mix	Sample	1 Day	3 Days	7 Days	28 Days
1	1	3704	4997	5635	5904
	2	3753	4874	5486	5774
	3	n/a	n/a	5277	5858
2	1	3079	4252	5449	6105
	2	3532	4568	5177	6035
	3	3289	4208	5279	5816
3	1	2936	4135	4730	5712
	2	2875	4334	5062	6015
	3	3939	4036	n/a	6123
4	1	3089	4301	4856	5775
	2	2451	4055	4672	5603
	3	2963	4214	4919	4866
5	1	2496	3760	4389	5460
	2	2509	3704	4128	5313
	3	2409	3477	4508	4751

1 psi = 6.89 kPa

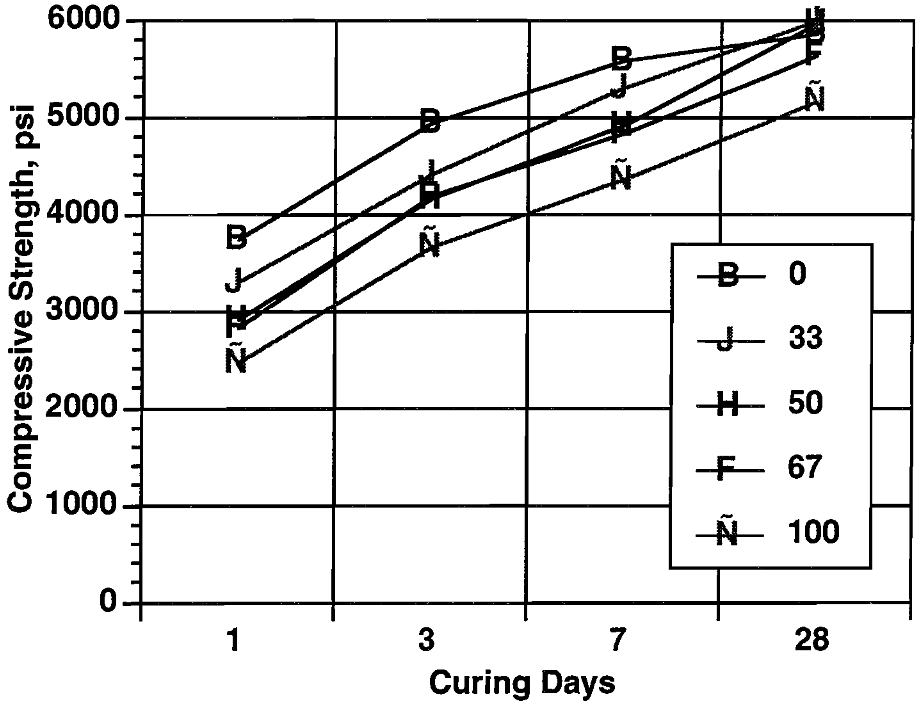

1 psi = 6.89 kPa

Figure 4.2 Compressive strength (psi) (Note: Values in legend refer to percent SRG)

Table 4.2 Splitting tensile strength (psi)

Mix	Sample	1 Day	3 Days	7 Days	28 Days
1	1	352	384	575	538
	2	401	465	453	503
	3	400	360	-	500
2	1	332	425	490	548
	2	327	526	497	553
	3	410	463	539	555
3	1	303	483	398	296
	2	222	423	402	451
	3	269	494	445	589
4	1	296	446	476	55
	2	332	416	500	441
	3	349	422	493	510
5	1	298	388	452	493
	2	291	353	477	482
	3	253	302	445	426

1 psi = 6.89 kPa

MODULUS OF ELASTICITY (E)

Concrete modulus of elasticity was tested after the same curing period used in the previous two tests. Following the procedure specified in ASTM C-469 (Ref 14), elastic moduli were calculated from longitudinal deformations under continuous compressive loading using the following equation:

$$E = \frac{(S_2 - S_1)}{(e_2 - 0.00005)}$$

where:

E = chord modulus of elasticity (psi),

S_2 = 40 percent ultimate stress value,

S_1 = stress corresponding to strain of 50 millionths (psi), and

e_2 = longitudinal strain produced by stress S_2.

Results appear in Table 4.3 and in Figure 4.4.

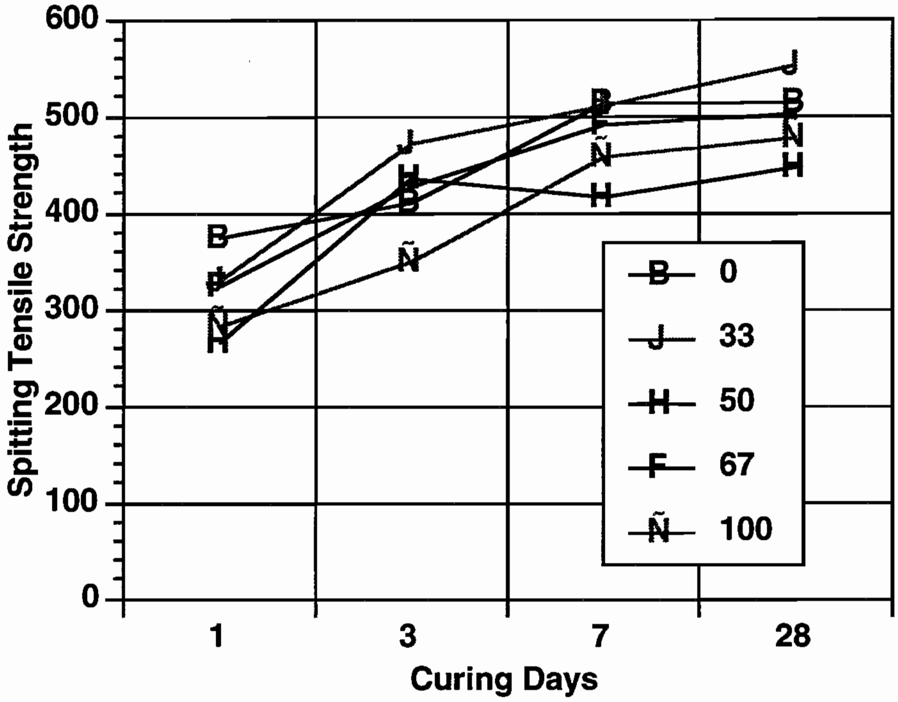

Figure 4.3 Splitting tensile strength (Note: Values in legend refer to percent SRG)

COEFFICIENT OF THERMAL EXPANSION (A_C)

Coefficient of thermal expansion was measured after 56 days, using the method described in ASTM C-531 (Ref 14). This test involves measuring each specimen at 22.78°C (73°F), heating the specimens in a moisture-controlled environment to 48.89°C (120°F), measuring their length again, and then cooling them back to 22.78°C (73°F) and measuring them a final time. The relative humidity was held constant at 40 percent throughout the test. The test was repeated three times on the same specimens. The coefficient of thermal expansion was then calculated as follows:

$$C = (Z-Y-W)/T(W-X)$$

where:

Z = length of bar, including studs, at elevated temperature (in.),

Y = length of stud expansion (in.) = X x T x k (where k is the linear coefficient of thermal expansion per °F of the studs)

W = length of bar, including studs, at lower temperature (in),

T = temperature change (°F),

X = length of the two studs at lower temperature (in.), and

k = 9.6 $\mu\varepsilon$/°F.

Table 4.3 Modulus of elasticity (psi, millions)

Mix	Sample	1 Day	3 Days	7 Days	28 Days
1	1	2.8210	2.9796	3.4587	2.9976
	2	2.3553	3.2206	3.1846	2.8360
	3	1.9940		2.8758	2.9328
2	1	2.8875	3.1256	3.6241	3.6686
	2	2.8140	3.1901	3.3303	3.6396
	3	2.5047	2.7420	3.8636	4.1298
3	1	3.132	3.8832	3.9312	4.1455
	2	2.8649	3.2977	3.578	4.0308
	3	3.1093	3.4532	3.8847	4.2483
4	1	3.1769	3.3431	4.2179	4.4698
	2	2.4056	3.3153	3.7571	4.2904
	3	3.3273	3.5824	3.8115	4.1273
5	1	3.2264	3.4918	3.8804	4.5825
	2	3.0467	3.5577	4.2058	4.9604
	3	2.9059	3.4635	4.0695	4.5241

1 psi = 6.89 kPa

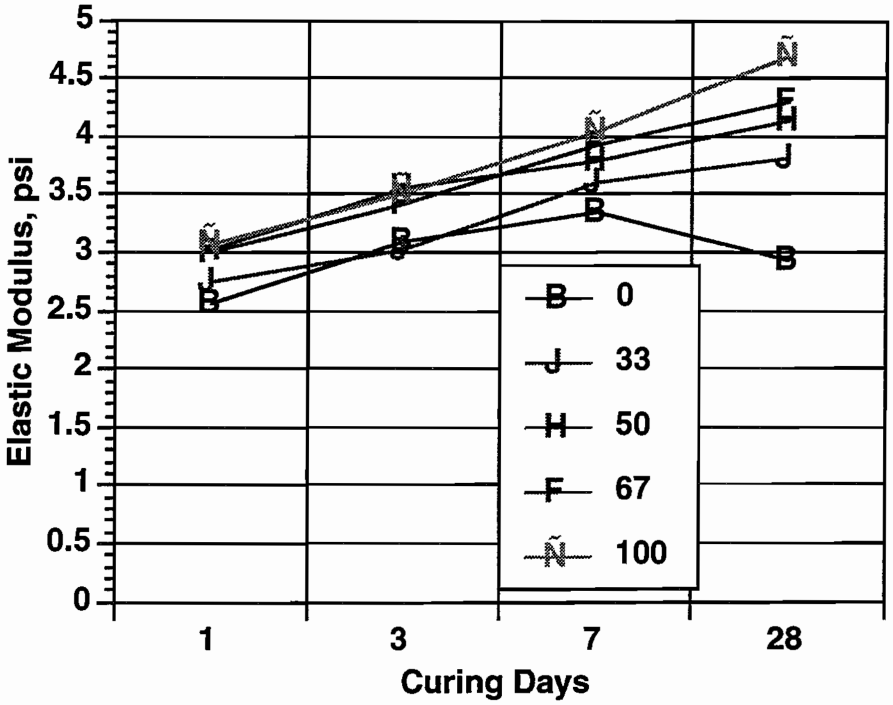

1 psi = 6.89 kPa

Figure 4.4 Modulus of elasticity (Note: Values in legend refer to percent SRG)

Table 4.4 Coefficient of thermal expansion (1/°F)

Mix	Sample 1	Sample 2	Sample 3	Average
1	3.8866	2.7810	4.0740	3.5805
2	4.0600	4.2854	3.2437	3.8630
3	3.7384	3.6705	2.5429	3.3173
4	4.8003	3.9531	4.2417	4.3317
5	4.9159	5.3621	3.8644	4.7141

°C=5/9(°F-32)

DISCUSSION OF RESULTS

Using the results of the laboratory experiment, we are updating and refining the computer programs developed at the Center for Transportation Research (CTR) of The University of Texas at Austin. From previous testing, as discussed earlier, mathematical models were developed to use a chemical analysis of an aggregate's oxides to predict the five properties studied in all three phases. These equations were used to develop the program CHEM. Using the prediction information, the mix designer would be able to determine if the aggregate was acceptable for use in the pavement, without having to wait on lengthy lab testing for results. If the aggregate was not acceptable, the designer could then consider a blend with a second aggregate that was of better quality. From there, the user would repeat the prediction steps before turning to the design program, CRCP-7, also developed at CTR. Normalized curves from the laboratory experiment results will enable the CRCP-7 program to be updated to include the design of pavements using blends of two aggregates. Currently, the program requests information about one aggregate and other pertinent pavement design information. Chapters 5 will discuss in further detail the CRCP and CHEM programs, and how the Phase II testing will be adapted for inclusion.

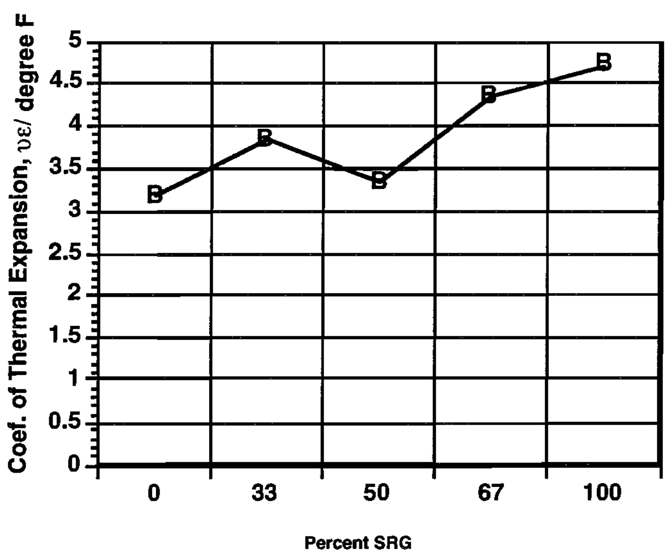

°C=5/9(°F-32)

Figure 4.5 Coefficient of thermal expansion

CHAPTER 5. DATA ANALYSIS

The hypothesis underlying this research is that concrete made with a blend of two aggregates will exhibit properties that differ from those of single-aggregate concrete. In this study, we limited the aggregates to two types, namely, crushed limestone and siliceous river gravel. The properties evaluated, as discussed in Chapter 4, were compressive strength, splitting tensile strength, elastic modulus, and coefficient of thermal expansion. This chapter discusses the data analysis undertaken to determine the relationship between the properties of single-aggregate concretes and blended-aggregate concretes.

STATISTICAL ANALYSIS

The first relationship evaluated was the linear relationship (which is also the most desirable). If a property varied linearly with the percentage of the blend, a hypothesized equation could be expressed as follows:

$$f(\text{blend}) = f(\text{SRG}) + [\{f(\text{LS})-f(\text{SRG})\}\text{x}(\%\text{LS}/100)] \qquad \text{(Eq. 5.1)}$$

where:

$f(\text{blend})$ = property value of a mix with blended aggregates,
$f(\text{SRG})$ = property value of a mix with 100% siliceous river gravel,
$f(\text{LS})$ = property value of a mix with 100% crushed limestone, and
$\%\text{LS}$ = percent crushed limestone.

Using the statistical program SAS, the results of the laboratory experiment were analyzed using statistical regression methods to produce a best-fit equation. The regression results were as follows:

Compressive Strength: $\text{CS(blend)} = 1.013(\text{SRG})+0.960(\text{Product})$
$R^2 = 99\%$ (Eq. 5.2)
Splitting Tensile Strength: $\text{TS(blend)} = 1.013(\text{SRG})+0.796(\text{Product})$
$R^2 = 99\%$ (Eq. 5.3)
Elastic Modulus: $\text{EM(blend)} = 1.009(\text{SRG})+1.092(\text{Product})$
$R^2 = 99\%$ (Eq. 5.4)
Thermal Expansion: $\text{TE(blend)} = 1.014(\text{SRG})+1.083(\text{Product})$
$R^2 = 92\%$ (Eq. 5.5)

where:

$$\text{product} \; = \; [\{f(\text{LS})-f(\text{SRG})\}\text{x}(\%\text{LS}/100)].$$

Each equation was very close to being linear. Figures 5.1 through 5.4 graphically compare the statistical and linear equations. Each property had two data sets consisting of different aggregate sources for the limestone and river gravel. In both cases, the results proved to be almost linear. Though the amount of data used to draw this conclusion is very limited, the variation between the best-fit equations and the linear equations are minimal enough to conclude that the relationship between single aggregate concretes and blended aggregate concretes is linear.

OTHER FACTORS AFFECTING RESULTS

There were other factors affecting the results that were not considered in the analysis. One such factor was curing method. To better compare laboratory and field results, Project 422/1244 researchers had determined that lab tests should be undertaken at 23.3°C (74 °F) and at 40 percent relative humidity. As a result of an oversight on the part of the laboratory experiment designer, however, the samples tested in Phase II were moist-cured from the day cast to the day tested (e.g., samples tested at three days were moist-cured for three days).

Another factor affecting the results was mixing quality. Because the concrete batches were prepared by inexperienced students, the aggregate types were not adequately mixed in the laboratory. Rather than blend the aggregates before adding to the cement mixer, the students blended the aggregates in the mixer before adding sand, cement, water, and admixture. Mix 1, 100 percent limestone of Group 1, was remixed as Mix 6 for this reason. Specimens were therefore screened for any discontinuities in the concrete, though no obvious problems were noted.

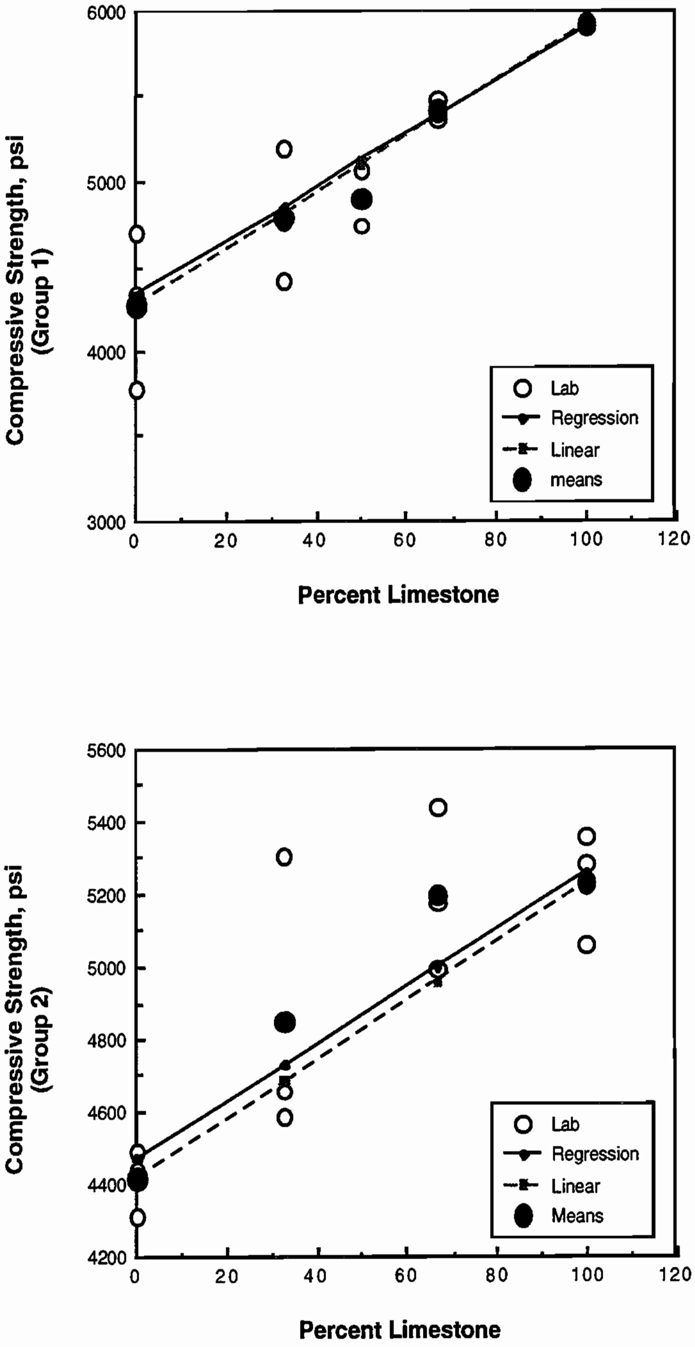

Figure 5.1 Compressive strength analysis (psi=6.89 kPa)

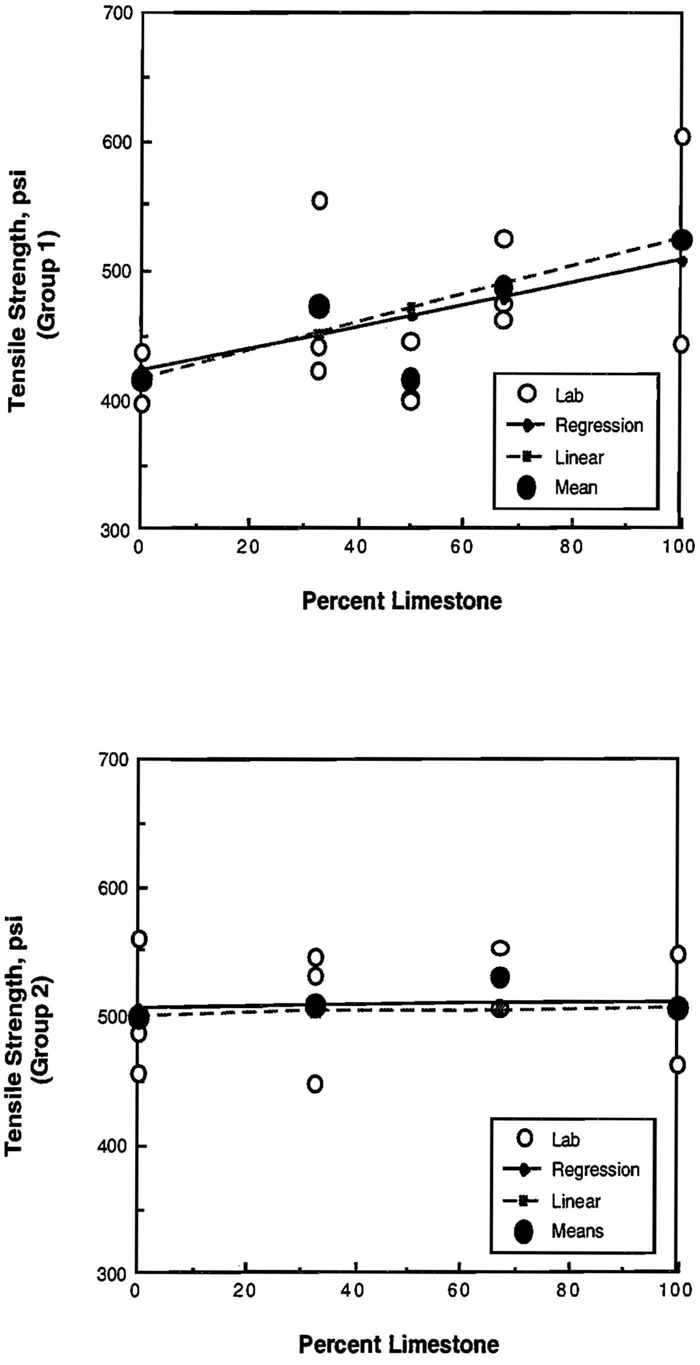

Figure 5.2 Splitting tensile strength analysis (psi=6.89 kPa)

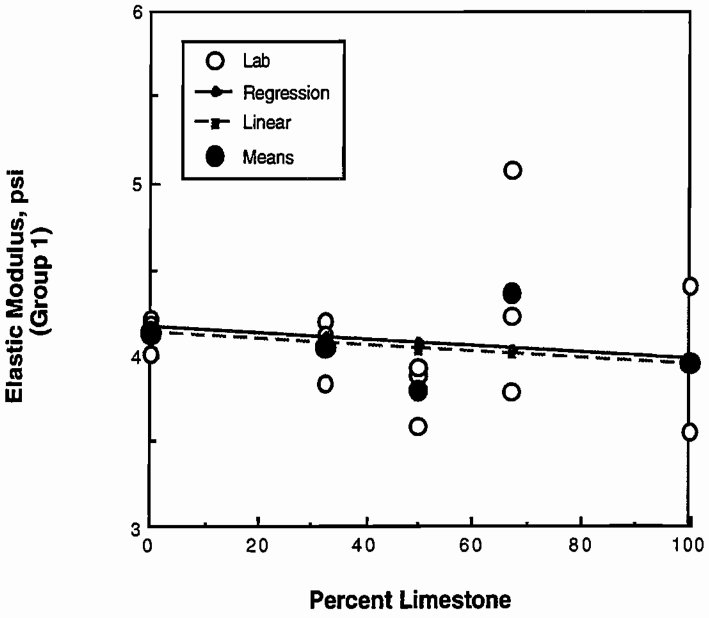

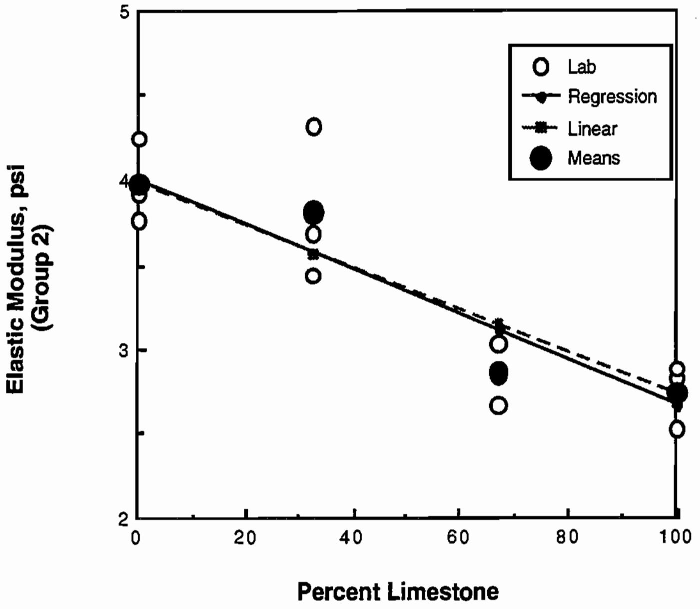

Figure 5.3 Elastic modulus analysis (psi=6.89 kPa)

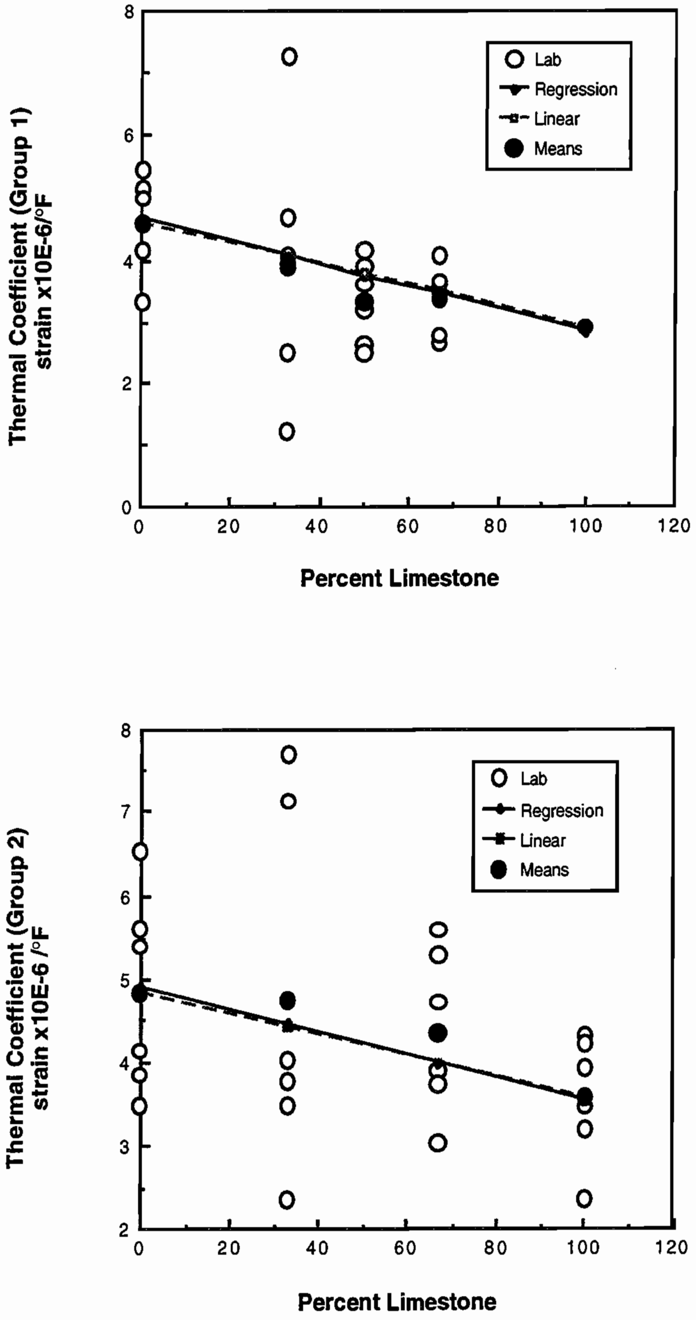

Figure 5.4 Coefficient of thermal expansion analysis

CHAPTER 6. IMPLEMENTATION

PREVIOUS RESEARCH

From Phase I and Phase II testing, normalized models were developed to estimate the tensile strength, compressive strength, and modulus of elasticity of portland cement concrete at a curing time, t, relative to a chosen "final" curing time, t_f, of 28 days, as discussed in Chapter 1. The result was the following equation (Eq. 1.1):

$$F_N(t) = N_{28}(2 - e^{-Bt} - e^{-Ct})$$

where:

t = the time of curing (days), and

N_{28}, B, and C = coefficients of curvature specific to each aggregate, given in Table 1.1.

Equation 1.1, which ranges from 0 at t = 0 to 1 at t = 28, should be used to calculate normalized tensile strength, compressive strength, and elastic modulus of a concrete with a singular aggregate type. The results of the equation can then be multiplied by a 28-day property value to yield a predicted value for time t. If the 28-day property value is unknown, it can be predicted by using the CHEM program mentioned earlier. Through a simple chemical analysis of an unknown aggregate, chemical composition in percentages can be obtained. These can be input into the CHEM program for prediction of 28-day values of a property.

PREDICTING PROPERTIES OF BLENDED AGGREGATES

The properties of blended aggregates can be estimated by, first, using Eq. 1.1 to predict for each aggregate source, and then taking a weighted average of the results. For example, the predicted compressive strength of a concrete made with SRG at a time of 7 days would be calculated as follows:

$$F_c(7) = N_{28}(2 - e^{-Bt} - e^{-Ct})$$

$$F_c(7) = 0.5020(2 - e^{-(0.182)(7)} - e^{-(0.473)(7)})$$

$$F_c(7) = 0.8453$$

Thus, the 7-day compressive strength value is estimated to be 84.53 percent of the 28-day value. Applying the equation to SRG and LS aggregates with known 28-day strengths, the compressive strength for a blended aggregate concrete can be predicted as follows:

For SRG: $F_c(7) = 0.8453 \times 4909 = 4149$ psi

For LS: $F_c(7) = 0.7758 \times 5845 = 4534$ psi

For 75% LS / 25% SRG: $F_c(\text{blend}) = 4149 + [\{4534 - 4149\}(0.75)]$

$F_c(\text{blend}) = 4438$ psi

(Note: psi=6.89 kPa)

In this manner, a mix designer can obtain a reasonable idea of the properties of the blended aggregate concrete without having to go through a time-consuming and costly lab testing procedure. This concept is the basis for predicting aggregate blend performance in the CHEM and CRCP programs.

DETERMINATION OF BLENDING RATIO

These equations might also be useful in determining the desired blending ratio by calculating in the opposite direction. For example, if a specification is for a property such as compressive strength, an engineer could first predict the value for an aggregate to determine if it will be acceptable; if it is not, a blend could be considered. The equations could be used as follows to determine the required blending ratio for the project:

Predicted f_c for aggregate X = 4297 psi
Predicted f_c for aggregate Y = 5012 psi
Desired f_c for blend = 4800 psi
$f_c(\text{blend}) = f_c(X) + [\{f_c(Y) - f_c(X)\}x(\%Y)]$
$4800 = 4297 + [\{5012-4297\}x(\%Y)]$
$\%Y = 70$
(Note: psi=6.89 kPa)

Thus, it is predicted that if 70 percent of aggregate Y is used, the desired value for compressive strength may be obtained. This blending ratio should be evaluated for other critical properties (such as thermal coefficient or drying shrinkage) to ensure that it meets the necessary minimum or maximum values. If all values are met, a mix should be tested in the laboratory for confirmation of the property values. If all values are not met, the mix should be re-evaluated for a proper blend.

THE CHEM2 PROGRAM

In order to easily apply the chemical prediction models and aggregate blending relationships, a computer program, CHEM2, has been developed for the IBM PC and its compatibles (Fig 6.1). CHEM2 is an improved version of CHEM1 (Ref 7), which was developed through the limestone and river gravel aggregate testing in Phase I of this project. Both CHEM1 and CHEM2 input the percentage by weight of certain oxide residues produced by standard fusion testing, predicting f_t, f_c, E, and Z for curing times ranging from 1 to 28 days. Although both programs provide a rough prediction of material properties for concrete made with a new aggregate source prior to actual laboratory testing, CHEM2 features improved models based on mineral content; it also estimates properties for blended aggregates.

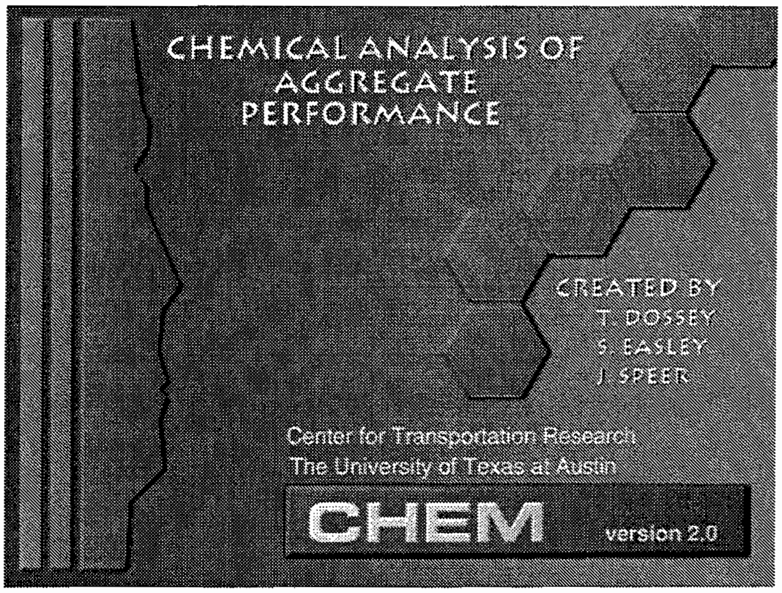

Figure 6.1 The CHEM2 Program for the IBM PC

The overall purpose for predicting concrete material properties for various aggregates is to determine the design parameters (steel percent, bar size, etc.) needed to obtain a desired level of pavement performance. With design tools such as the CRCP programs (Ref 5), these factors can be estimated. If the concrete material properties are known, they can be directly input into the concrete performance programs; if not, the properties can be estimated using the CHEM2 procedure and then transferred to the performance programs. In this way, it is hoped that equal and adequate performance from very different aggregates can be obtained.

Improved Models for Limestones and River Gravels

CHEM2 obtains improved results by first identifying the type of aggregate and then predicting performance using a model specifically developed for that aggregate class. This is especially important for aggregate types that produce similar oxide residues (e.g., SRG and granite, both high in SiO_2) but differ in mineral composition and, therefore, exhibit characteristic differences when cast in concrete. The program can either identify the class of aggregate by direct user input, or determine it through a simple set of "IF" statements based on the oxide test results. Once the class is determined, the original mineral content is first back-calculated from the oxide residue stoichiometrically (Ref 20).

Since limestones and river gravels are the primary focus of the overall study, special attention has been given to these aggregates. As described in Chapter 4, the two new limestone and two new river gravel aggregates that were tested have added enough additional data to make more type-specific models possible. These models can now estimate differences in strength, elastic modulus, shrinkage, and thermal expansion based on small differences in the characteristic minerals composing the aggregates, presumably calcium carbonate (Ca_2CO_3) and dolomite ($CaMgCO_3$) for limestone, and quartz (SiO_2) for river gravel.

Prediction of Thermal Coefficient

CHEM2 predicts thermal coefficient of expansion. This is a vitally important property, particularly for pavements placed in the summer season, when temperature extremes are high and when peak ambient temperature may coincide with peak heat of hydration (as in morning placements). Under such conditions, for a given steel design, a high thermal coefficient tends to produce more closely-spaced early-age cracking, compared with an aggregate with a lower coefficient.

Despite the desirability of such a model, problems with using the oxide residues directly previously prevented the development of a definitive model. This difficulty has been overcome by first back-calculating the original mineral content. Although it was hoped that the additional thermal coefficient testing in the Phase III experiment would provide additional data to further improve the thermal coefficient model, the values were consistently low compared with the Phase I and II testing and with other results in the literature. CHEM2 currently predicts thermal coefficient based on the Phase II data.

Predictions for Aggregate Blends

CHEM2 also adds a facility for predicting the performance of blended aggregates. As documented in Chapter 5, an experiment to determine the effect of blending limestone with river gravel at various proportions was conducted. This experiment was designed to reveal the shape of the "blending curves" (Fig 4.1), which could then be normalized for each material property and used to predict the performance of blends. Initially, it was not known whether the properties of a blended aggregate could be described by the weighted average for the two aggregates (Fig 6.2, curve A, linear) or by some non-linear combination (Fig 6.2, curve B & C). The results given in Chapter 5 conclusively support curve A, the simple linear combination. CHEM2 therefore determines the properties for blended aggregates by estimating for each individual aggregate and then taking a weighted average according to the blending ratio.

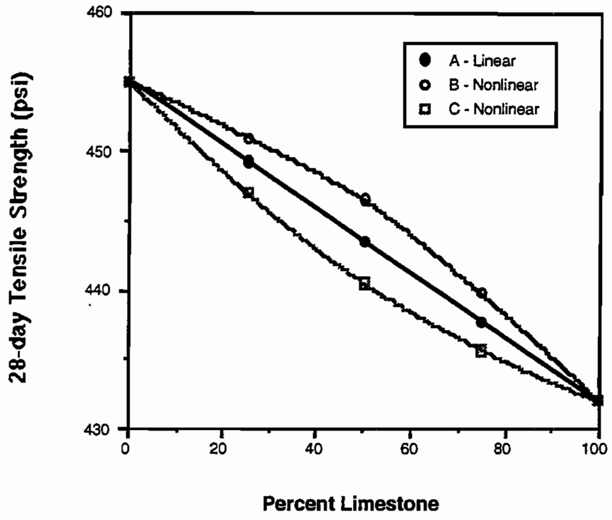

Figure 6.2 Possible performance shapes for aggregate blends (psi=6.89 kPa)

Program Flow

The CHEM2 program operates as follows: (1) User input of chemical composition data is obtained, (2) prediction models for the five material properties are produced, (3) potential problem areas are highlighted (e.g., excessively high thermal coefficient), and (4) at the user's option, a second screen is produced predicting the performance of the original aggregate blended at any ratio with a standard or user-input limestone (Fig 6.3). These graphs can be printed once the approximate blending level is determined that will produce material properties resulting in the desired level of performance.

Stoichiometric Analysis

One of the problems encountered in the development of the CHEM1 models was that only the oxide residues were considered as predictors. Since different minerals may break down into different oxides of the same compound (e.g., dolomite and calcite both contribute to the calcium oxide residue), direct empirical modeling based on oxide residue is problematic. Therefore, a methodology was developed for back-calculating the percentage by weight of the various minerals that compose the aggregates used in the Phase II study. Mineral composition determined in this way can then be used to develop more robust predictive models for such aggregate-dependent concrete properties as tensile strength, compressive strength, elastic modulus, drying shrinkage, and thermal coefficient of expansion.

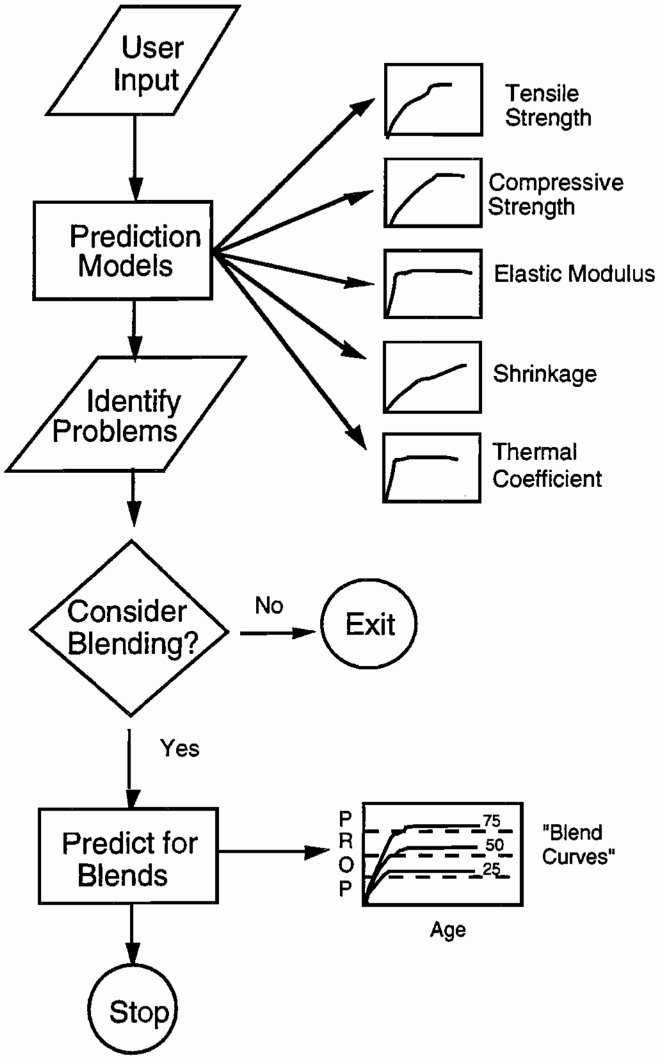

Figure 6.3 CHEM2 Program flow

Problems with Previous Chemical Models

Phase II testing under this project collected aggregate chemical composition data for eight aggregates commonly used in Texas pavements, and for a number of additional aggregates (Ref 7). Several analytical procedures were performed, including determination of principal mineral composition by x-ray diffraction, and oxide residue analysis after fusion.

Dossey and McCullough (Ref 7) document an effort to predict aggregate performance based solely on oxide residues. Although some useful models were developed, some of the models were later determined to have weak predictive ability outside the inference space of the eight tested aggregates. The problem with oxide-based models is that few of the oxides measured actually existed in the aggregate prior to chemical testing; in fact, most of the oxides were formed by the break down of more complex minerals in the sample. For example, little if any calcium oxide (CaO) was present in the aggregate prior to fusion; most was produced by the oxidation of calcite (limestone, $CaCO_3$), with an additional amount coming from dolomite ($CaMg(CO_3)_2$).

This situation reveals a fundamental problem: Since the amount of each oxide is proportional not to a single mineral but to several, no strong direct correlation is observed between oxide percentage and concrete material properties. The models developed in the reference attempt to compensate by considering interactions. These interactions serve as surrogate variables or indirect indicators for the original mineral content of the sample.

Methodology

A much better method is to develop models based directly on the original mineral composition of the aggregates. Fortunately, stoichiometric analysis (Ref 20) can be used to back-calculate these percentages.

Using the results from x-ray crystallography (Table 6.1), the principal minerals in each aggregate sample are determined. Most are composed primarily of calcite ($CaCO_3$), quartz (SiO_2), and/or dolomite ($CaMgCO_3$). A notable exception is Scotland Granite, which contains a substantial amount of the sodium feldspar albite ($Na_2O \bullet Al_2O_3 \bullet 6SiO_2$). It is the albite (and other feldspars) in granite that cause it to be an outlying point in much of the previous analysis. For instance, the granite (GR) and Vega (VG) aggregates tested had thermal coefficients of 5.7 and 6.5 microstrains/°F, respectively; yet GR has an SiO_2 residue of 71.3 vs. 66.9 percent for VG. Since quartz is so thermally expansive, this is counter-intuitive. Because the break down of albite yields additional SiO_2, granite appears to have had the second highest mineral quartz content of the tested aggregates; however this is not the case. Much of the SiO_2 residue came from albite, not quartz. Albite and quartz have very different physical properties (e.g., thermal coefficient of expansion). The technique presented here will eliminate this type of problem.

Table 6.1 Mineral composition of Phase II aggregates

Minerals Found				
Source	Aggregate Type	Most Abundant	Second	Third
McCelligan # 1	DL	Dolomite	Calcite	Quartz
Western-Tascosa	WT	Quartz	Calcite	
Tin-Top # 1	BTT	Calcite	Quartz	
Bridgeport	BTT	Calcite	Dolomite	Quartz
Feld (TCS)	LS	Calcite	Dolomite	Quartz
Fordyce	SRG	Quartz	Calcite	
Vega	VG	Quartz	Calcite	
Ferris # 1	FR	Calcite	Quartz	
Scotland Granite	GR	Quartz	Albite	

Assumptions

Mined aggregate is a complex blend of many minerals. It would be impossible from the rudimentary information given in Table 6.1 to determine the exact mineral composition of the aggregates. Fortunately, a methodology to back-calculate the principal minerals should be all that is needed to develop more robust models. Accordingly, the following imprecise but essentially correct assumptions were made:

1) All SiO_2 residue in the sample came from quartz or feldspar (granite is composed of quartz and feldspar). Only the commonly occurring feldspars, albite (the sodic plagioclase feldspar), orthoclase and microcline (potassium feldspars, chemically $K_2O{\bullet}Al_2O_3{\bullet}6SiO_2$) were considered in this analysis. Orthoclase and microcline have the same chemical composition but differ in crystalline structure.
2) All CaO residue in the sample came from calcite or dolomite.

Reactions

These two assumptions imply the following decompositions:

$CaCO_3 \rightarrow CaO + CO_2$ (Eq. 6.1) calcite

$CaMg(CO_3)_2 \rightarrow MgO + CaO + 2CO_2$ (Eq. 6.2) dolomite

$Na_2OAl_2O_3{\bullet}6SiO_2 \rightarrow 6SiO_2 + Al_2O_3 + Na_2O$ (Eq. 6.3) albite

$K_2OAl_2O_3{\bullet}6SiO_2 \rightarrow 6SiO_2 + Al_2O_3 + K_2O$ (Eq. 6.4) potassium feldspars

Computational Method — Carbonates

Using the molecular weights for the compounds (Table 6.2), along with the balanced equations above, one can easily determine the weight ratios relating the oxides to the original mineral content. For instance, from Eq. 6.2 it can be seen that dolomite breaks down into MgO in a 1-to-1 ratio. That is, each mole of dolomite produces one mole of magnesium oxide. Since the molecular weight of dolomite is 184.407 and the molecular weight of MgO is 40.305, then 184.407/40.305 = 4.575 grams of dolomite must have existed for each gram of MgO in the original sample.

$$\text{dolomite (g)} = \text{MgO (g)} \bullet 4.5752 \qquad \text{(Eq. 6.6)}$$

Table 6.2 Molecular weights for selected compounds

Compound	Molecular Weight (g)
Calcite	100.091
Dolomite	184.407
Quartz	60.0855
Albite	524.48
Kalinite	546.674
CaO	56.08
MgO	40.305
SiO_2	60.086

In order to estimate the original calcite in the sample, it is first necessary to subtract the amount of CaO produced from dolomite (CaO_{dol}). The decomposition of dolomite yields CaO in a 1:1 molar ratio, or 56.08g CaO / 184.407 g dolomite = 0.3041.

$$CaO_{dol}\ (g) = \text{dolomite}\ (g) \bullet 0.3041 \qquad \text{(Eq. 6.7)}$$

Then, CaO from the decomposition of calcite (CaO_{cal}) equals the total CaO (CaO_{tot}) less the amount released from dolomite:

$$CaO_{cal}\ (g) = CaO_{tot}\ (g) - CaO_{dol}\ (g) \qquad \text{(Eq. 6.8)}$$

Now that CaO_{cal} is known, the original percent calcite (limestone) can be calculated. In a 1:1 ratio, 1 mole (100.091g) of calcite produces 1 mole (56.08) of CaO, giving a molecular weight ratio of 100.091/56.08 = 1.785.

$$\text{calcite}\ (g) = CaO_{cal}\ (g) \bullet 1.785 \qquad \text{(Eq. 6.9)}$$

Computational Method — Silicates

A similar process can be employed to determine the original silicate content. First, assuming most or all Na_2O was produced by the break down of albite (see Table 6.1), the following formula is given:

$$\text{albite (g)} = \text{Na}_2\text{O (g)} \bullet 8.46 \qquad \text{(Eq. 6.10)}$$

Assuming most or all K_2O was produced by the breakdown of potassium feldspars (PF), such as orthoclase and microcline:

$$\text{PF (g)} = \text{K}_2\text{O (g)} \bullet 5.8 \qquad \text{(Eq. 6.11)}$$

Calculating SiO_2 from albite ($SiO_{2(alb)}$):

$$\text{SiO}_{2(\text{alb})}\text{ (g)} = \text{albite (g)} \bullet 0.6874 \qquad \text{(Eq. 6.12)}$$

Calculating SiO_2 from potassium feldspars ($SiO_{2(PF)}$):

$$\text{SiO}_{2(\text{PF})}\text{ (g)} = \text{PF (g)} \bullet 0.6595 \qquad \text{(Eq. 6.13)}$$

Then the remaining SiO_2 must have been quartz prior to testing:

$$\text{quartz (g)} = \text{SiO}_{2(\text{tot})}\text{ (g)} - \text{SiO}_{2(\text{alb})}\text{ (g)} - \text{SiO}_{2(\text{pf})}\text{ (g)} \qquad \text{(Eq. 6.14)}$$

Results

Percentages after decomposition for the eight aggregates are given in Table 6.3. A computer program was used to calculate mineral content according to Eqs. 6.6-6.14. The results of running this program on the oxide residue data are given in Table 6.4. As a check of the methodology, the remaining unexplained mineral content is given as a column in the table.

Table 6.3 Phase II chemical analysis results

Source	Aggregate Type	Type	SiO_2	CaO	MgO	CO_2	MnO	Fe_2O_3	Al_2O_3	Na_2O	K_2O	TiO_2	Other
McKelligan	Dolomite	(DL)	6.53	34.9	13.0	42.9	.02	0.21	0.38	0.09	0.26	0.02	1.69
Western-T	S/L	(WT)	68.5	11.4	0.35	8.98	.05	2.64	3.97	0.85	1.1	0.17	1.99
Bridpt+TinTop	L+S/L	(BTT*)	17.53	42.55	0.71	35.65	0.04	0.57	0.56	0.15	0.30	0.04	1.91
Feld (TCS)	Limestone	(LS)	2.56	45.7	5.97	43.3	.01	0.06	0.21	0.14	0.21	0.02	1.82
Fordyce	SRG	(SRG)	93.8	2.23	0.11	1.77	.01	0.76	0.63	0.18	0.32	0.1	0.09
Vega	SRG	(VG)	66.9	11.6	0.39	9.07	.07	2.33	4.22	0.95	1.16	0.19	3.12
Ferris	L/S	(FR)	14.2	42.1	0.43	34.4	.10	3.70	0.87	0.17	0.26	0.06	3.71
Scotland	Granite	(GR)	71.3	1.5	0.63	0.59	.03	1.52	14.3	4.4	3.83	0.29	1.61

*These aggregates combined in a 50/50 blend when tested in the laboratory for concrete properties.

Table 6.4 Calculated mineral composition, percent by weight

Aggregate	Calcite	Dolomite	Quartz	Albite	PF	Unexplained
BTT	73.98	3.245	15.51	1.269	1.77	4.23
DL	29.87	59.42	5.01	0.76	1.54	4.3
FR	73.87	1.97	12.22	1.44	1.54	8.96
GR	1.11	2.88	31.05	37.23	22.63	5.1
LS	66.53	27.29	0.94	1.18	1.24	2.82
SRG	3.70	0.50	91.53	1.52	1.89	0.86
VG	19.68	1.78	56.93	8.04	6.86	6.71
WT	19.42	1.60	59.35	7.19	6.50	5.94

Discussion

In general, the procedure performs very well in describing the mineral content of the original sample. No conflict was found with the original crystallography analysis (Table 6.1). Most of the oxide residue was accounted for, with a maximum of 8.96 percent unexplained for aggregate (FR). This is probably owing to the large amount of ferric minerals found in this aggregate that were not addressed in the analysis.

THERMAL COEFFICIENT MODEL

Using the estimated mineral content from the stoichiometric procedure (Table 6.3), regression was used to model the thermal coefficient of expansion for concrete (α_c) as a function of mineral content in the sample:

$$\alpha_C = e^{1.098} \bullet (\text{Quartz})^{0.486} \bullet (\text{Calcite})^{-0.106} \bullet (\text{Dolomite})^{0.415} \bullet (\text{PF})^{-2.37} \bullet (\text{Albite})^{1.635} \qquad \text{(Eq. 6.15)}$$

where:

Quartz = % quartz by weight,

Calcite = % calcite by weight,

Dolomite = % dolomite by weight,

PF = % potassium feldspars by weight,

Albite = % albite by weight, and

FS = Albite + PF, all feldspars by weight.

Figure 6.4 shows the fit for the thermal coefficient model. This model has been tested on several additional aggregates and provides reasonable predictions in most cases. Additional models for tensile strength, compressive strength, and elastic modulus were also fit by a similar method:

$$f_c = e^{8.943} \bullet (\text{Calcite})^{-0.086} \bullet (\text{Quartz})^{-0.072} \bullet (\text{Dolomite})^{-0.021} \bullet (\text{Feldspars})^{-0.033} \qquad \text{(Eq. 6.16)}$$

$$f_t = 1298 - 8.87 \bullet (\text{Calcite}) - 8.089 \bullet (\text{Quartz}) - 7.45 \bullet (\text{Dolomite}) - 49.8 \bullet (\text{PF}) + 16.6 \bullet (\text{Albite}) \qquad \text{(Eq. 6.17)}$$

$$E = e^{1.115} \bullet (\text{Calcite})^{-0.0087} \bullet (\text{Quartz})^{0.121} \bullet (\text{Dolomite})^{0.088} \bullet (\text{Feldspars})^{-0.101} \qquad \text{(Eq. 6.18)}$$

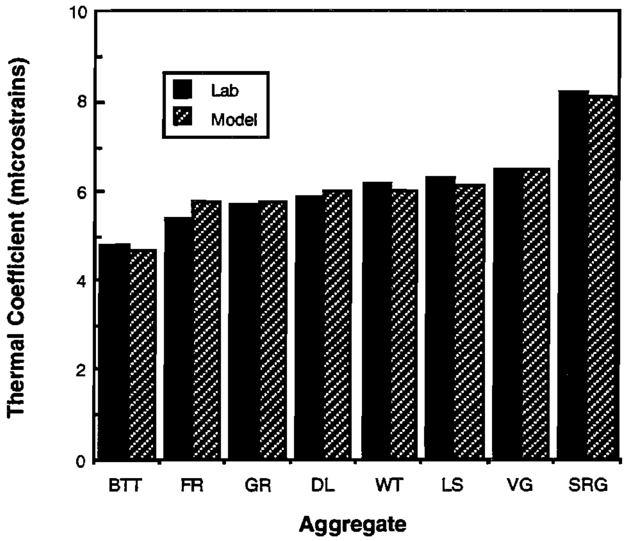

Figure 6.4 Fit for thermal coefficient model (Eq. 6.15)

It must be stressed that the models were developed using only the Phase II laboratory data (eight Texas aggregates) and thus are very restricted in terms of inference space. In the future, it is hoped that additional aggregate testing will expand the CHEM2 database and improve the model. In particular, as suggested earlier, additional siliceous and limestone aggregate data are needed to improve the blending model.

USING THE CHEM2 PROGRAM

As mentioned earlier, all of the equations and models developed in this report have been incorporated into a computer program capable of running on IBM PCs and compatibles. The minimum computer requirements to run CHEM2 include a VGA color monitor and 8.89-cm (3 1/2-inch) disk drive. The program itself requires only about 400K of memory, so there are no special requirements in memory or hard drive storage. At present, the program runs under DOS 3.0 or better and does not require WINDOWS.

To run the program, the user first inputs the oxide residue values obtained from the standard fusion analysis described earlier. These values are percent by weight, and must add up to less than or equal to 100 percent. Normally, the chemical analysis will not identify all of the sample, so the unexplained portion is calculated by the program and reported as “Other” (Fig 6.5).

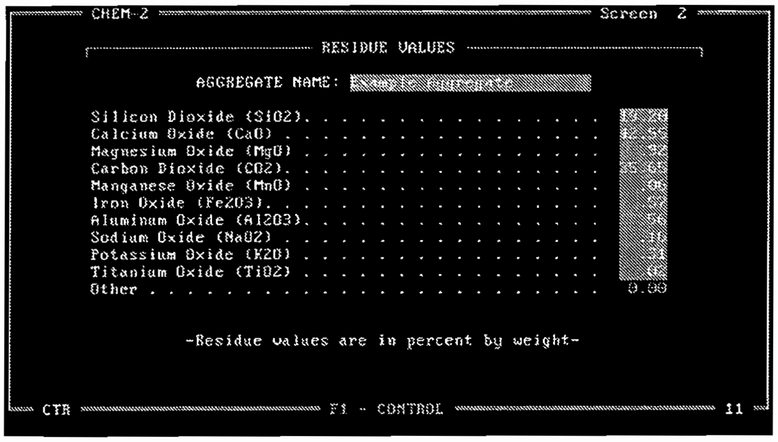

```
CHEM-2                                                    Screen 2

                          RESIDUE VALUES

              AGGREGATE NAME: Example Aggregate

       Silicon Dioxide (SiO2). . . . . . . . . . . . . . . .  [illegible]
       Calcium Oxide (CaO) . . . . . . . . . . . . . . . . .  [illegible]
       Magnesium Oxide (MgO) . . . . . . . . . . . . . . . .  [illegible]
       Carbon Dioxide (CO2). . . . . . . . . . . . . . . . .  [illegible]
       Manganese Oxide (MnO) . . . . . . . . . . . . . . . .  [illegible]
       Iron Oxide (Fe2O3). . . . . . . . . . . . . . . . . .  [illegible]
       Aluminum Oxide (Al2O3). . . . . . . . . . . . . . . .  [illegible]
       Sodium Oxide (NaO2) . . . . . . . . . . . . . . . . .  [illegible]
       Potassium Oxide (K2O) . . . . . . . . . . . . . . . .  [illegible]
       Titanium Oxide (TiO2) . . . . . . . . . . . . . . . .  [illegible]
       Other . . . . . . . . . . . . . . . . . . . . . . . .    0.00

              -Residue values are in percent by weight-

CTR                       F1 - CONTROL                                11
```

Figure 6.5 CHEM2 data entry screen

If blending calculations are desired, the user must input properties for the limestone that will be used (Fig 6.6). Aggregates other than limestone may be used for blending, but the shape of the time curves used internally in the program have been optimized for limestone. If the tensile strength, compressive strength, elastic modulus, drying shrinkage, and thermal coefficient of the blending limestone are not known, the limestone can be tested chemically and CHEM2 can be used to estimate these properties as well.

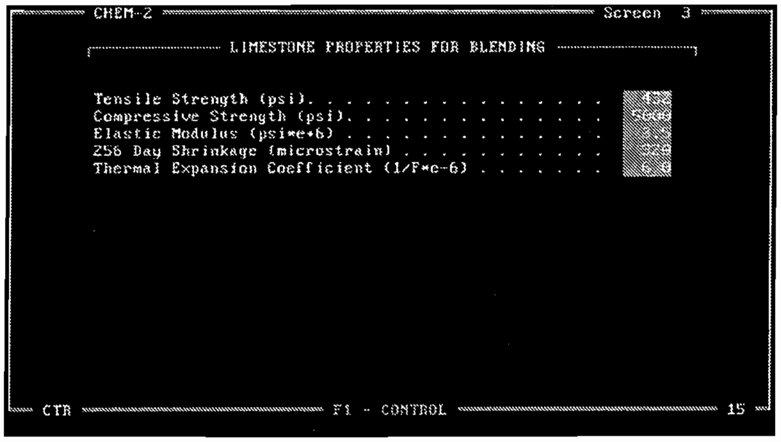

```
CHEM-2                                              Screen  3
        LIMESTONE PROPERTIES FOR BLENDING

Tensile Strength (psi). . . . . . . . . . . . . . . .
Compressive Strength (psi). . . . . . . . . . . . . .
Elastic Modulus (psi*e+6) . . . . . . . . . . . . . .
256 Day Shrinkage (microstrain) . . . . . . . . . . .
Thermal Expansion Coefficient (1/F*e-6) . . . . . . .

CTR                      F1 - CONTROL                   15
```

Figure 6.6 CHEM2 limestone properties screen

The oxide residue values, together with the blending limestone properties, comprise a worksheet that may be saved by the program for further work. This facility is provided so that the user may retrieve a previously saved set of data to try a different blending ratio. This may be necessary if the CRCP5 analysis program predicts poor performance of the blended aggregate. Pressing F1 activates the control menu, which can be used to save or retrieve worksheets (Fig 6.7).

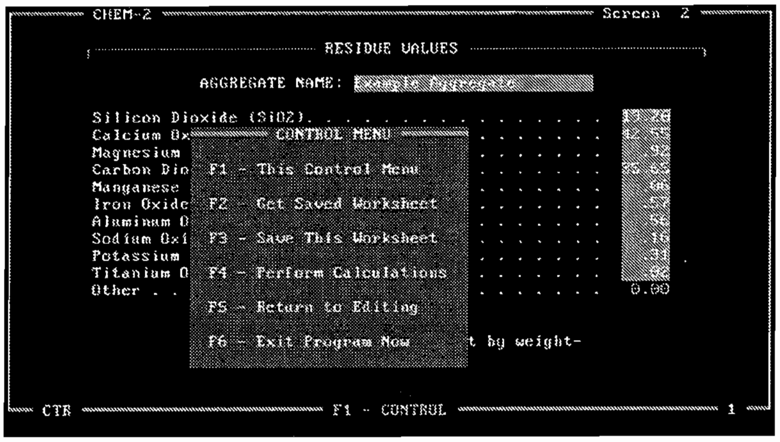

```
CHEM-2                                              Screen  2
                 RESIDUE VALUES

          AGGREGATE NAME:

Silicon Dioxide (SiO2). . . . . . . . . . . . . . . .
Calcium Ox  ═══ CONTROL MENU ═══  . . . . . . . .
Magnesium                          . . . . . . . .
Carbon Dio   F1 - This Control Menu . . . . . . . .
Manganese                          . . . . . . . .
Iron Oxide   F2 - Get Saved Worksheet . . . . . . .
Aluminum O                         . . . . . . . .
Sodium Oxi   F3 - Save This Worksheet . . . . . . .
Potassium                          . . . . . . . .
Titanium O   F4 - Perform Calculations . . . . . . .
Other . .                          . . . . . . . .   0.00
             F5 - Return to Editing

             F6 - Exit Program Now      t by weight-

CTR                      F1 - CONTROL                   1
```

Figure 6.7 CHEM2 control menu

From the control menu, the analysis is run by pressing the F4 key. The program will back-calculate the original mineral content by the procedure delineated above and display the results in the form of a bar graph. The time-dependent material properties are displayed in graphical format at the bottom right of the screen. Using the F1 key now pages between the various material property predictions (Fig 6.8).

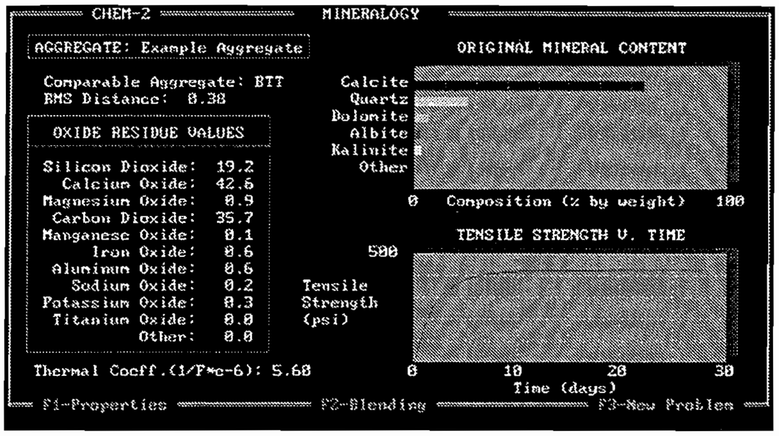

```
AGGREGATE: Example Aggregate

Comparable Aggregate: BTT
RMS Distance:  0.38

OXIDE RESIDUE VALUES

 Silicon Dioxide:  19.2
   Calcium Oxide:  42.6
 Magnesium Oxide:   0.9
  Carbon Dioxide:  35.7
 Manganese Oxide:   0.1
      Iron Oxide:   0.6
  Aluminum Oxide:   0.6
    Sodium Oxide:   0.2
 Potassium Oxide:   0.3
  Titanium Oxide:   0.0
           Other:   0.0

Thermal Coeff.(1/F*e-6): 5.60
```

Figure 6.8 CHEM2 output screen

Pressing F2 changes to the aggregate blending screen. By adjusting the limestone content, the properties of the blend can be adjusted anywhere between the test aggregate properties and the pure limestone properties. In this way, the designer can determine the optimal blending ratio needed to attain the desired concrete properties. Finally, these properties can be input into the CRCP or JRCP analysis programs on the concrete property screen to predict pavement performance.

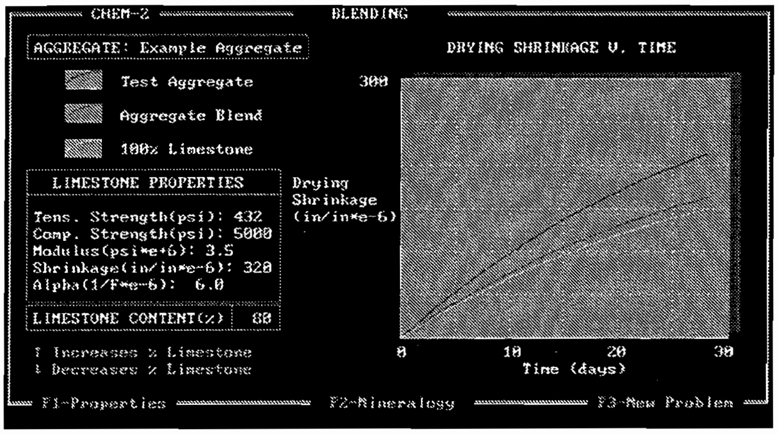

```
AGGREGATE: Example Aggregate

LIMESTONE PROPERTIES

Tens. Strength(psi): 432
Comp. Strength(psi): 5000
Modulus(psi*e+6): 3.5
Shrinkage(in/in*e-6): 320
Alpha(1/F*e-6):  6.0

LIMESTONE CONTENT(%) | 80
```

Figure 6.9 CHEM2 blending prediction screen

SUMMARY

The models given here for thermal coefficient, compressive strength, tensile strength, and elastic modulus are approximate and not intended to replace actual field and laboratory testing of concrete material properties. However, the stoichiometric methodology developed (CHEM2) is a significant improvement over direct regression techniques using oxide residue analysis (e.g. CHEM1). As more data become available, the regression models predicting concrete performance from aggregate mineral content can be continually improved until they are able to predict reliably over a wider range of aggregate types.

CHEM2 offers the pavement designer the opportunity to estimate the performance of new, untried aggregates before undergoing the expense of full concrete testing. At the time of this writing, the oxide residue test needed to run CHEM2 costs less than $100.

CHAPTER 7. SUMMARY AND RECOMMENDATIONS

SUMMARY

This chapter presents, first, the conclusions of the Phase III testing and, second, some recommendations for further research into the area of aggregate blending. This project has had two main objectives: (1) investigate the effect of blended coarse aggregates on portland cement concrete pavements, and (2) develop a methodology for designing similarly performing portland cement concrete pavements from a variety (i.e., a blend) of coarse aggregate sources.

Earlier efforts in this project studied the effects of aggregates on portland cement concrete. These efforts were limited to unblended, or single-aggregate, concrete. The results showed that aggregates did have a strong effect on the performance of pavements constructed with portland cement concrete. Some of the causative factors identified included aggregate type/physical properties, aggregate thermal properties/chemical properties, aggregate strength/mechanical properties, and the interaction of aggregate type with the time of construction. Of all the pavements tested, those constructed of siliceous river gravel performed more poorly than those pavements constructed with crushed limestone (especially in situations where high temperature differentials existed during paving). The results were attributed to the gravel's high coefficient of thermal expansion. However, this study shows that portland cement concrete made with a blend of siliceous river gravel and crushed limestone can mitigate some of the gravel's adverse properties.

At the beginning of the experiment, it was unknown whether concrete properties with blended aggregates would follow a simple linear trend between unblended aggregate concretes, or if they would be defined by a more complex shape. For each of the four properties tested in this project (i.e., compressive strength, elastic modulus, splitting tensile strength, and coefficient of thermal expansion), a hypothesized linear mathematical model was compared with a model developed from a regression analysis. For each, the linear model was hypothesized as follows (Eq. 5.1):

$$f(\text{blend}) = f(\text{SRG}) + [\{f(\text{LS})-f(\text{SRG})\}x(\%\text{LS}/100)]$$

where:

f(blend) = property value of a mix with blended aggregates,

f(SRG) = property value of a mix with 100% siliceous river gravel,

f(LS) = property value of a mix with 100% crushed limestone, and

%LS = percent crushed limestone.

Despite significant experimental scatter, the means of all four regression best-fit equations followed along the linear hypothesized equations. The r^2 (coefficient of determination) values varied from 92 percent for the coefficient of thermal expansion, to 99 percent for compressive strength. These r^2 values represent the proportionate reduction of total variation associated with the use of the independent variables. Thus, the larger r^2 is, the more the total variation is reduced (Ref 19).

Even though the experiment was limited to four aggregate samples and one curing method, the experimental results demonstrate conclusively that blended aggregate properties vary linearly in proportion with the blending ratio of the aggregate types used.

RECOMMENDATIONS

Aggregate blending should be used to mitigate undesirable concrete properties, such as high thermal coefficient of expansion. In this way, pavement engineers can use coarse aggregates that would otherwise be unsuitable under certain paving conditions (e.g., high daily temperature variation). Also, equal performance can be obtained from pavements constructed with very different coarse aggregates. Further research encompassing other aggregate types is necessary before the CRCP and CHEM design tools can be combined into a functional, operating procedure. However, from the research conducted in this study, the following recommendations can be made:

- blending of coarse aggregates should be performed during concrete mixing to ensure even blending;
- the linear weighted averaging technique presented here should be developed as a computer tool to assist designers in previewing the performance of a blended aggregate mix design prior to laboratory concrete testing;
- additional sources for both crushed limestone and siliceous river gravel should be tested to further expand the database for the CRCP and CHEM programs, ensuring accurate predictions of properties for unknown aggregate and aggregate blends; and
- further testing of aggregates other than limestone and siliceous river gravel should be conducted to expand and refine the aggregate property prediction equations and to confirm the linearity of blends of other aggregate types.

With the refinement of the blend models from further research, properties can be accurately estimated for any ratio of crushed limestone and siliceous river gravel where properties of the pure aggregates are known. Using estimates from the newly developed models, designers will be able to go one step further by using currently established design tool programs, such as HIGHWAY, to determine how the predicted blend will affect pavement properties, thus producing equal pavement performance.

REFERENCES

1. Dolar-Mantuani, Ludmila, *Handbook of Concrete Aggregates: A Petrographic and Technological Evaluation,* National Research Council of Canada, 1983.
2. Dossey, Terry, Humberto Castedo, and B. Frank McCullough, "Prediction of Concrete Properties Using Coarse Aggregate Chemical Composition Data," *Transportation Research Record No. 1284, Materials and Construction; Cement, Admixtures, and Concrete 1990,* National Research Board, 1990.
3. Barksdale, Richard D., (ed.), *The Aggregate Handbook,* National Stone Association, 1991.
4. Guiterrez de Velasco, M., and B. F. McCullough, "Summary Report for 1978 CRCP Condition Surveys in Texas," Report 177-20, Center for Transportation Research, University of Texas at Austin, January 1981.
5. Won, M. C., "Mechanistic Analysis of Continuously Reinforced Concrete Pavements Considering Materials Characteristics, Variability and Fatigue," doctoral dissertation, Department of Civil Engineering, University of Texas at Austin, May 1989.
6. Hankins, Kenneth, Young Chan Suh, and B. Frank McCullough, "Field Investigation of Coarse Aggregate Types: Criteria for Test Sections," Research Report 422/1244-1, Center for Transportation Research, The University of Texas at Austin, January 1991.
7. Dossey, Terry, and B. Frank McCullough, "Characterization of Concrete Properties with Age," Research Report Number 422/1244-2, Center for Transportation Research, The University of Texas at Austin, March 1992.
8. Suh, Young Chan, B. F. McCullough, and Ken Hankins, "Development and Application of Randomness Index for Continuously Reinforced Concrete Pavement," Research Report 422/1244-3, Center for Transportation Research, The University of Texas at Austin, March 1992.
9. Jimenez, Miguel Angel Ortero, B. Frank McCullough, and Kenneth Hankins, "Monitoring of Siliceous River Gravel and Limestone Continuously Reinforced Concrete Pavement Test Sections in Houston 2 Years After Placement, and Development of a Crack Width Model for CRCP-7 Program," Research Report Number 1244-4, Center for Transportation Research, The University of Texas at Austin, March 1992.
10. Kosmatka, S. H., and William C. Panarese, *Design and Control of Concrete Mixes*, Portland Cement Association, 13th ed., 1988.
11. Texas State Department of Highways and Public Transportation, *Manual of Testing Procedures-Physical Section*, Texas State Department of Highways and Public Transportation, 1987.
12. Mehta, P. Kumar, "Concrete: Structure, Properties and Materials," Prentiss-Hall, 1986.
13. Perloff, William H., and William Baron, "Soil Mechanics: Principles and Applications," John Wiley & Sons, 1976.

14. *Annual Book of ASTM Standards,* 1980, 1985, 1991, Section 4, Construction, Vol. 04.02, Concrete and Mineral Aggregates.

15. Freedman, J., "Properties of Materials for Reinforced Concrete," in *Handbook of Concrete Engineering*, M. Fintel (ed.), New York: Van Nostrand Reinhold Company, 1987.

16. Barow, R. S., "The Effect of Fly Ash on the Temperature Rise in Concrete," Master's thesis, The University of Texas at Austin, 1988.

17. Neter, John, William Wasserman, and Michael H. Kutner, *Applied Linear Statistical Models,* Richard D. Irwin, Inc., Homewood, IL, 1990.

18. Stoker, H. Stephen, *Introduction to Chemical Principles,* 2nd ed., MacMillan Publishing, 1986.

APPENDIX A:

GLOSSARY

GLOSSARY

Physical Properties: Physical properties of a material identify or describe it in terms of the fundamental dimensions of length, mass and time.

1. Particle Shape is the shape of the individual aggregate particle; shapes are described as cubic, blade, disc, or rod.
2. Maximum Particle Size is the minimum size screen opening through which 100 percent of the material will pass.
3. Particle Surface Texture is the degree of roughness or irregularity of the surface of an aggregate particle.
4. Pore Structure is defined by the size, volume, and shape of the void spaces (both permeable and impermeable) within an aggregate particle.
5. Porosity is the percentage of total volume of an aggregate particle occupied by pore spaces.
6. Permeability is the capacity of an aggregate particle, or a group of particles, to transmit fluid.
7. Specific Gravity is the ratio of the mass of a given volume of aggregate to the mass of an equal volume of water.
8. Thermal Conductivity is the ability of an aggregate to transmit heat.
9. Grading is the distribution of different particles of an aggregate by size.
10. Thermal Volume Change is the change in the volume of aggregate produced by a variation in temperature.
11. Thermal Conductivity is the ability of an aggregate to transmit heat.

Chemical Properties: Chemical properties identify a material chemically and indicate the transformation that a material undergoes as a result of a chemical process.

1. Solubility is the tendency of an aggregate to be dissolved by a liquid.
2. Slaking is the crumbling of an aggregate into visible particles when water or other liquids destroy the bond between its mineral grains and cause expansion of air inside the pores.
3. Base Exchange is the replacement of one type of cation adsorbed on the aggregate surface by another type of cation.
4. Surface Charge is the distribution of electric charges on the surface of an aggregate.

5. Coatings are deposits of mineral and / or chemical substances on the surface of an aggregate particle; such deposits may include clay, precipitated salts, or dust.

6. Oxidation Potential is the ability of an aggregate to react with atmospheric oxygen to produce oxides.

7. Chloride Content is the concentration of chloride ions present in aggregate particles.

8. Resistance to Attack by Chemicals is the ability of an aggregate to resist deteriorating attacks from such chemicals as deicing salts.

9. Chemical Compound Reactivity is the change in the structure of an aggregate produced by chemical reactions with the binder.

Mechanical Properties: Mechanical properties identify the behavioral characteristics of a material when it is subjected to an externally applied force.

1. Strength is the magnitude of tensile and compressive stress that an individual aggregate particle can withstand before failure occurs.

2. Resistance to Loads is the ability of an aggregate to resist polishing or being worn away by rubbing or friction.

3. Elastic Modulus is the resistance of an aggregate to deformation. It is also called particle stiffness or resilient modulus.

4. Resistance to Degradation is the ability of an aggregate to resist breakdown into smaller particles when subjected to applied forces (e.g., mixer blades or wheel loads).

Descriptions of Minerals: Minerals are strictly defined as naturally occurring chemical elements or compounds formed as a product of inorganic processes (Hurlbut, 1963). Rocks are composed of an assemblage of one or more distinct minerals. This definition of minerals excludes shells, coral, and other organically formed materials that otherwise are important constituents of some limestones. For the purpose of this report, these components are also considered to be minerals.

1. Elements consist of chemical elements that occur in nature in an uncombined state. Examples include sulfur, graphite, and gold.

2. Sulfides include combinations of various metallic elements with sulfur. An example is pyrite.

3. Oxides contain a metal element in combination with oxygen. The iron mineral hematite is an example. A subgroup within the oxides is the hydroxides, which include oxygen in the form of the hydroxyl radical or water. Limonite is an example of a hydroxide.

4. Halides are naturally occurring chlorides, fluorides, bromides, and iodides. Examples are halite (rock salt) and fluorite.

5. Carbonates contain the carbonate radical. The common minerals calcite and dolomite are included here.

6. Phosphates are minerals whose composition includes the phosphate radical. One example is apatite.

7. Sulfates include the sulfate radical. Gypsum is an example of a common sulfate mineral.

8. Silicates form the largest group of minerals. They contain various elements in combination with silicon and oxygen. Examples are quartz and feldspar.

APPENDIX B:

LABORATORY TESTING DATA

Sources

Group 1:

Texas Crushed Stone	LS	Georgetown, TX
Pioneer Aggregates	SRG	Eagle Lake, TX

Group 2:

Young Brothers	LS	Mexia, TX
LaGrange Aggr & Conc	SRG	LaGrange, TX

Laboratory Method

Properties:

Compressive Strength	ASTM C 39
Splitting Tensile Strength	ASTM C 496
Elastic Modulus	ASTM C 469
Coefficient of Thermal Expansion	ASTM C 531 (Modified)

Test Mixes:

All mixes were designed the same with only the coarse aggregate varying.

24 cylinders per mix (nom. 15.24 cm dia. x 30.48 cm, or 6" dia. x 12")
3 bars per mix (nom. 10.16 cm x 10.16 cm x 30.48 cm, or 4" x 4" x 12")

Testing:

Tests were conducted for compressive strength, splitting tensile strength, and elastic modulus on 1, 3, 7 and 28 days.

Thermal expansion measurements were taken after 56 days.

GROUP 1 DATA

Compressive Strength (avg), psi (psi=6.89 kPa)

Day	100 / 0	67 / 33	50 / 50	33 / 67	0 / 100
1	3488	3214	2917	3048	2605
3	4902	4579	4168	4624	3791
7	5912	5405	4896	4783	4271
28	-	6341	5950	6201	5411

Splitting Tensile Strength (avg), psi (psi=6.89 kPa)

Day	100 / 0	67 / 33	50 / 50	33 / 67	0 / 100
1	335	251	265	358	300
3	400	460	434	495	347
7	523	487	415	472	416
28	-	576	445	507	465

Elastic Modulus (avg), x 10^6 psi (psi=6.89 kPa)

Day	100 / 0	67 / 33	50 / 50	33 / 67	0 / 100
1	3.0590	3.1325	3.0350	3.2344	3.3121
3	3.5582	3.4373	3.5447	3.7487	3.7377
7	3.9502	4.3621	3.7980	4.0483	4.1328
28	-	4.3761	4.1415	4.5829	5.1185

Coefficient of Thermal Expansion, 1/ °F (°C=5/9[°F-32])

	100 / 0	67 / 33	50 / 50	33 / 67	0/100
a_c	2.9045	3.3554	3.3172	3.9186	4.5885

Mix Design, lb/yd^3 (lb/yd^3 = .59 kg/m^3)

	100 / 0	67 / 33	50 / 50	33 / 67	0 / 100
cement	492	492	492	492	492
water	221	221	221	221	221
LS	1820	1219	910	600	0
SRG	0	589	910	1216	1815
sand	1281	1326	1334	1351	1385
AEA (oz)	2.94	2.96	2.94	2.95	2.95
w/c	0.45	0.45	0.45	0.45	0.45

MIX 1 DATA
100% LS / 0% SRG

Compressive Strength, psi (psi=6.89 kPa)

Specimen	Day 1	Day 3	Day 7	Day 28
1	2419	2848	4013	5095
2	2525	3032	3616	4975
3	2465	3712	4431	5106
avg	2470	3197	5059	5059

Splitting Tensile Strength, psi (psi=6.89 kPa)

Specimen	Day 1	Day 3	Day 7	Day 28
1	310	N/A	429	399
2	218		387	514
3	235		469	585
avg	254		428	499

Elastic Modulus, x10^6 psi (psi=6.89 kPa)

Specimen	Day 1	Day 3	Day 7	Day 28
1	2.6018	2.7467	3.1958	3.6643
2	2.1232	3.8026	3.4111	3.7921
3	2.6638	3.4401	-	3.5830
avg	2.4629	3.1891	3.3035	3.6798

Coefficient of Thermal Expansion (avg), 1/°F (°C=5/9[°F-32])

a_c	2.9045

MIX 2 DATA
(67% LS / 33% SRG)

Compressive Strength, psi (psi=6.89 kPa)

Specimen	Day 1	Day 3	Day 7	Day 28
1	3275	4236	5468	6396
2	3077	4922	5362	6376
3	3289	-	5384	6251
avg	3214	4579	5405	6341

Splitting Tensile Strength, psi (psi=6.89 kPa)

Specimen	Day 1	Day 3	Day 7	Day 28
1	248	390	474	595
2	253	555	461	583
3	-	434	525	550
avg	251	460	487	576

Elastic Modulus, x 10^6 psi (psi=6.89 kPa)

Specimen	Day 1	Day 3	Day 7	Day 28
1	3.2594	3.5853	4.2261	4.6768
2	3.3440	3.9180	3.7921	4.1199
3	2.7942	2.8086	5.0680	4.3316
avg	3.1325	3.4373	4.3621	4.3761

Coefficient of Thermal Expansion, 1/°F (°C=5/9[°F-32])

Trial	Specimen 1	Specimen 2	Specimen 3	Average
1	3.6144	3.6220	2.7612	3.33
2	2.6298	4.0438	3.4612	3.38
Average				3.3554

MIX 3 DATA

(50% LS / 50% SRG)

Compressive Strength, psi (psi=6.89 kPa)

Specimen	Day 1	Day 3	Day 7	Day 28
1	2936	4135	4730	5712
2	2875	4334	5062	6015
3	2939	4036	-	6123
avg	2917	4168	4896	5950

Splitting Tensile Strength, psi (psi=6.89 kPa)

Specimen	Day 1	Day 3	Day 7	Day 28
1	303	483	398	296
2	222	423	402	451
3	269	494	445	589
avg	265	434	415	445

Elastic Modulus, x10^6 psi (psi=6.89 kPa)

Specimen	Day 1	Day 3	Day 7	Day 28
1	3.1320	3.8832	3.9312	4.1455
2	2.8649	3.2977	3.5780	4.0308
3	3.1093	3.4532	3.8847	4.2483
avg	3.0350	3.5447	3.7980	4.1415

Coefficient of Thermal Expansion, 1/°F (°C=5/9[°F-32])

Trial	Specimen 1	Specimen 2	Specimen 3	Average
1	3.5988	3.1806	2.4732	3.08
2	3.8779	4.1603	2.6125	3.55
Average				3.3172

MIX 4 DATA

(67% LS / 33% SRG)

Compressive Strength, psi (psi=6.89 kPa)

Specimen	Day 1	Day 3	Day 7	Day 28
1	3386	4735	4409	6190
2	2367	4413	4759	6211
3	3391	4724	5182	-
avg	3048	4624	4783	6201

Splitting Tensile Strength, psi (psi=6.89 kPa)

Specimen	Day 1	Day 3	Day 7	Day 28
1	284	540	422	590
2	408	442	554	413
3	383	504	440	519
avg	358	495	472	507

Elastic Modulus, x10^6 psi (psi=6.89 kPa)

Specimen	Day 1	Day 3	Day 7	Day 28
1	3.3174	3.5818	4.1199	4.8753
2	2.5123	3.6257	3.8373	4.5420
3	3.8736	4.0387	4.1876	4.3316
avg	3.2344	3.7487	4.0483	4.5829

Coefficient of Thermal Expansion, 1/°F (°C=5/9[°F-32])

Trial	Specimen 1	Specimen 2	Specimen 3	Average
1	7.2754	3.8561	1.2248	4.12
2	4.6525	2.4640	4.0387	3.72
Average				3.9186

MIX 5 DATA
(0% LS / 100% SRG)

Compressive Strength, psi (psi=6.89 kPa)

Specimen	Day 1	Day 3	Day 7	Day 28
1	2590	3825	4341	5796
2	2604	3725	3772	5611
3	2620	3825	4700	4824
avg	2605	3791	4271	5411

Splitting Tensile Strength, psi (psi=6.89 kPa)

Specimen	Day 1	Day 3	Day 7	Day 28
1	268	300	417	523
2	342	431	396	446
3	290	310	436	426
avg	300	347	416	465

Elastic Modulus, x10^6 psi (psi=6.89 kPa)

Specimen	Day 1	Day 3	Day 7	Day 28
1	3.5718	3.6208	4.0061	4.8024
2	3.1271	3.7962	4.1753	6.0223
3	3.2373	3.7962	4.2187	4.5309
avg	3.3121	3.7377	4.1328	5.1185

Coefficient of Thermal Expansion, 1/°F (°C=5/9[°F-32])

Trial	Specimen 1	Specimen 2	Specimen 3	Average
1	5.1408	4.5516	4.1446	4.61
2	5.4184	4.9684	3.3071	4.56
Average				4.5885

MIX 6 DATA
100% LS / 0% SRG

Compressive Strength, psi (psi=6.89 kPa)

Specimen	Day 1	Day 3	Day 7	Day 28
1	3485	4841	5916	N/A
2	3491	4962	5909	
avg	3488	4902	5912	

Splitting Tensile Strength, psi (psi=6.89 kPa)

Specimen	Day 1	Day 3	Day 7	Day 28
1	310	409	603	N/A
2	360	391	443	
avg	335	400	523	

Elastic Modulus, x10^6 psi (psi=6.89 kPa)

Specimen	Day 1	Day 3	Day 7	Day 28
1	3.1795	3.3729	4.3998	N/A
2	2.9384	3.7435	3.5505	
avg	3.0590	3.5582	3.9502	

Coefficient of Thermal Expansion, 1/°F (°C=5/9[°F-32])

N/A

GROUP 2 DATA

Compressive Strength (avg), psi (psi=6.89 kPa)

Day	100 / 0	67 / 33	33 / 67	0 / 100
1	3968	3386	2620	2338
3	4969	4230	3756	3502
7	5231	5197	4848	4412
28	5845	5629	5073	4909

Splitting Tensile Strength (avg), psi (psi=6.89 kPa)

Day	100 / 0	67 / 33	33 / 67	0 / 100
1	412	408	292	261
3	419	483	360	348
7	505	530	507	500
28	514	528	497	490

Elastic Modulus (avg), x10^6 psi (psi=6.89 kPa)

Day	100 / 0	67 / 33	33 / 67	0 / 100
1	2.0762	2.3383	2.7054	2.8072
3	2.6419	2.6011	3.0784	3.2709
7	2.7373	2.8499	3.8093	3.9704
28	2.9221	3.2488	4.0086	4.2594

Coefficient of Thermal Expansion, 1/°F (°C=5/9[°F-32])

LS / SRG	100 / 0	67 / 33	33 / 67	0 / 100
a_c	3.58	4.37	4.75	4.84

Mix Design, lb/yd^3 (lb/yd^3 = .59 kg/m^3)

LS / SRG	100 / 0	67 / 33	33 / 67	0 / 100
cement	492	492	492	492
water	229	221	222	223
LS	1690	1214	608	0
SRG	0	590	1215	1808
sand	1216	1320	1352	1383
AEA (oz)	2.81	2.96	2.96	2.95
w/c	.47	.45	.45	.45

MIX 7 DATA
100% LS / 0% SRG

Compressive Strength, psi (psi=6.89 kPa)

Specimen	Day 1	Day 3	Day 7	Day 28
1	3922	5153	5354	5904
2	-	4786	5062	5774
3	4014	-	5277	5858
avg	3968	4969	5231	5845

Splitting Tensile Strength, psi (psi=6.89 kPa)

Specimen	Day 1	Day 3	Day 7	Day 28
1	394	359	547	538
2	442	538	463	503
3	400	360	-	500
avg	412	419	505	514

Elastic Modulus, x10^6 psi (psi=6.89 kPa)

Specimen	Day 1	Day 3	Day 7	Day 28
1	2.4625	2.5862	2.5176	2.9976
2	1.7721	2.6976	2.8186	2.8360
3	1.9940	-	2.8758	2.9328
avg	2.0762	2.6419	2.7373	2.9221

Coefficient of Thermal Expansion, 1/°F (°C=5/9[°F-32])

Trial	Specimen 1	Specimen 2	Specimen 3	Average
1	3.466	2.3578	4.2165	3.35
2	4.3072	3.2041	3.9323	3.81
Average				3.58

MIX 8 DATA
(67% LS / 33% SRG)

Compressive Strength, psi (psi=6.89 kPa)

Specimen	Day 1	Day 3	Day 7	Day 28
1	2882	4267	5429	5813
2	3986	4213	4991	5693
3	3289	4208	5173	5380
avg	3386	4230	5197	5629

Splitting Tensile Strength, psi (psi=6.89 kPa)

Specimen	Day 1	Day 3	Day 7	Day 28
1	416	460	505	500
2	400	496	532	523
3	410	492	552	560
avg	408	483	530	528

Elastic Modulus, x10^6 psi (psi=6.89 kPa)

Specimen	Day 1	Day 3	Day 7	Day 28
1	2.5156	2.6658	3.0220	2.6591
2	2.2840	2.4621	2.8684	3.1592
3	2.2152	2.6753	2.6591	3.9280
avg	2.3383	2.6011	2.8499	3.2488

Coefficient of Thermal Expansion, 1/°F (°C=5/9[°F-32])

Trial	Specimen 1	Specimen 2	Specimen 3	Average
1	5.2780	5.5814	3.0276	4.36
2	4.7176	3.8942	3.7247	4.11
Average				4.37

MIX 9 DATA
(33% LS / 67% SRG)

Compressive Strength, psi (psi=6.89 kPa)

Specimen	Day 1	Day 3	Day 7	Day 28
1	2792	3866	5302	5359
2	2534	3697	4585	4994
3	2534	3704	4655	4866
avg	2620	3756	4848	5073

Splitting Tensile Strength, psi (psi=6.89 kPa)

Specimen	Day 1	Day 3	Day 7	Day 28
1	307	351	530	520
2	256	389	446	469
3	315	340	546	501
avg	292	360	507	497

Elastic Modulus, x10^6 psi (psi=6.89 kPa)

Specimen	Day 1	Day 3	Day 7	Day 28
1	3.0364	3.1043	4.3158	4.0643
2	2.2988	3.0048	3.6768	4.0387
3	2.7810	3.1260	3.4353	3.9229
avg	2.7054	3.0784	3.8093	4.0086

Coefficient of Thermal Expansion, 1/°F (°C=5/9[°F-32])

Trial	Specimen 1	Specimen 2	Specimen 3	Average
1	3.7784	2.3523	4.0280	3.39
2	3.4948	7.1399	7.6750	6.10
Average				4.75

MIX 10 DATA
(0% LS / 100% SRG)

Compressive Strength, psi (psi=6.89 kPa)

Specimen	Day 1	Day 3	Day 7	Day 28
1	2402	3694	4436	5036
2	2413	3683	4484	5014
3	2197	3129	4315	4677
avg	2338	3502	4412	4909

Splitting Tensile Strength, psi (psi=6.89 kPa)

Specimen	Day 1	Day 3	Day 7	Day 28
1	328	475	487	463
2	240	275	558	517
3	216	294	454	-
avg	261	348	500	490

Elastic Modulus, x10^6 psi (psi=6.89 kPa)

Specimen	Day 1	Day 3	Day 7	Day 28
1	2.8810	3.3627	3.7547	4.3625
2	2.9662	3.3192	4.2362	3.8984
3	2.5744	3.1308	3.9202	4.5172
avg	2.8072	3.2709	3.9704	4.2594

Coefficient of Thermal Expansion, 1/°F (°C=5/9[°F-32])

Trial	Specimen 1	Specimen 2	Specimen 3	Average
1	3.4924	5.4032	4.1425	4.35
2	5.6120	6.5251	3.8632	5.33
Average				4.84